

Article

Dimerized Linear Mimics of a Natural Cyclopeptide (TMC-95A) Are Potent Noncovalent Inhibitors of the Eukaryotic 20S Proteasome

Audrey Desvergne, Emilie Genin, Xavier Marechal, Nerea Gallastegui, Laure Dufau, Nicolas Richey, Michael Groll, Joelle Vidal, and Michèle REBOUD-RAVAUX

J. Med. Chem., **Just Accepted Manuscript** • DOI: 10.1021/jm4002007 • Publication Date (Web): 29 Mar 2013

Downloaded from <http://pubs.acs.org> on April 16, 2013

Just Accepted

“Just Accepted” manuscripts have been peer-reviewed and accepted for publication. They are posted online prior to technical editing, formatting for publication and author proofing. The American Chemical Society provides “Just Accepted” as a free service to the research community to expedite the dissemination of scientific material as soon as possible after acceptance. “Just Accepted” manuscripts appear in full in PDF format accompanied by an HTML abstract. “Just Accepted” manuscripts have been fully peer reviewed, but should not be considered the official version of record. They are accessible to all readers and citable by the Digital Object Identifier (DOI®). “Just Accepted” is an optional service offered to authors. Therefore, the “Just Accepted” Web site may not include all articles that will be published in the journal. After a manuscript is technically edited and formatted, it will be removed from the “Just Accepted” Web site and published as an ASAP article. Note that technical editing may introduce minor changes to the manuscript text and/or graphics which could affect content, and all legal disclaimers and ethical guidelines that apply to the journal pertain. ACS cannot be held responsible for errors or consequences arising from the use of information contained in these “Just Accepted” manuscripts.



1
2
3
4
5
6
7
8
9
10
11
12
13
14
15
16
17
18
19
20
21
22
23
24
25
26
27
28
29
30
31
32
33
34
35
36
37
38
39
40
41
42
43
44
45
46
47
48
49
50
51
52
53
54
55
56
57
58
59
60

Dimerized Linear Mimics of a Natural Cyclopeptide (TMC-95A) Are Potent Noncovalent Inhibitors of the Eukaryotic 20S Proteasome

Audrey Desvergne[†], Emilie Genin[‡], Xavier Maréchal[†], Nerea Gallastegui[§], Laure Dufau[†],

Nicolas Richy[‡], Michael Groll[§], Joëlle Vidal^{‡,}, Michèle Reboud-Ravaux^{†,*}*

[†]Enzymologie Moléculaire et Fonctionnelle, UR4, University Paris 6-Pierre et Marie Curie,
UPMC-Sorbonne Universités, case 256, 7 quai Saint Bernard, 75252 Paris Cedex 05, France

[‡]Université de Rennes 1, Chimie et photonique moléculaires, CNRS-UMR 6510, Bâtiment 10A,
Campus de Beaulieu, 35042 Rennes Cedex, France

[§]Center for Integrated Protein Science at the Department Chemie Lehrstuhl für Biochemie,
Technische Universität München, Lichtenbergstr. 4, 85747 Garching, Germany

ABSTRACT

Noncovalent proteasome inhibitors introduce an alternative mechanism of inhibition to that of covalent inhibitors used in cancer therapy. Starting from a noncovalent linear mimic of TMC-95A, a series of dimerized inhibitors using polyaminohexanoic acid spacers has been designed and optimized to target simultaneously two of the six active sites of the eukaryotic 20S proteasome. The homodimerized compounds actively inhibited chymotrypsin-like ($K_i = 6-11$ nM) and trypsin-like activities whereas post-acidic activity was poorly modified. The noncovalent binding mode was ascertained by X-ray crystallography of the inhibitors complexed with the yeast 20S proteasome. The inhibition of proteasomal activities in human cells was evaluated. The use of the multivalency inhibitor concept has produced highly efficient and selective noncovalent compounds (no inhibition of calpain and cathepsin) that have potential therapeutic advantages compared to covalently binding bortezomib and carfilzomib.

INTRODUCTION

The ubiquitin-proteasome system plays an essential role in nuclear and cytosolic protein degradation in eukaryotic cells by controlling numerous essential cellular processes including turnover and quality control of proteins, cell cycle and apoptosis, transcription and cell signaling, immune response and inflammation.^{1,2} The degradation of proteins is mediated by the constitutive 26S multicatalytic proteasome that consists of a 20S catalytic core and two 19S regulatory complexes. The catalysis of proteolysis is accomplished by the 20S proteasome particle that has been the major target to identify and develop inhibitors as potential drugs able to modulate proteasomal activity. The clinical value of proteasome inhibition has become evident since the FDA approval of bortezomib for the treatment of relapsed multiple myeloma and mantle cell lymphoma.³⁻⁵ This drug is a highly selective peptide boronate.⁶ Nevertheless, due in particular to the presence of the boronic acid moiety, prolonged treatments induce toxicity and severe adverse effects including neurological disorders.⁷⁻⁹ Resistances have also been reported.¹⁰ The main second-generation proteasome inhibitors that are in clinical trials are carfilzomib¹¹ (approved in July 2012 for treatment of multiple myeloma) (PR-171), marizomib¹² (salinosporamide or NPI-0052), ixazomib¹³ (MLN-9708), oprozomib¹⁴ (ONX-0912 or PR-047) and delanzomib¹⁵ (CEP-18770). As with bortezomib, they are all covalent binding inhibitors reacting with the catalytic threonine of the active sites to form a covalent adduct.¹⁶ Noncovalent inhibitors, which are devoid of a reactive group, do not have the drawbacks generally associated with the presence of a warhead, such as lack of specificity, instability and excessive reactivity, though epoxyketones are the most specific applied proteasome inhibitors to date. Since toxicity will always be an issue for proteasome inhibitors, because of the huge variety of functions implicating this proteolytic machinery, noncovalent proteasome inhibitors may be an alternative to covalent ones.^{4,17} This less documented category of inhibitors includes the natural cyclopeptide

1
2
3 **1** (TMC-95A)¹⁸ (Figure 1A) and simpler cyclic¹⁹⁻²¹ and linear mimics^{22,23} obtained by rational
4 drug design. Several series of peptide and pseudopeptide noncovalent inhibitors were identified
5 by *in vitro* screenings of small or very large synthetic chemical libraries coupled with chemical
6 optimization.²⁴⁻²⁹ Noncovalent hydroxyureas have also been recently identified by *in vitro*
7 screening³⁰ and *in silico* screening of a large collection of organic compounds led to several
8 structurally distinct noncovalent inhibitors.³¹ A growing number of studies suggest that
9 proteasome inhibitors may become valuable drugs for the treatment of non-tumorous diseases
10 when used in conditions in which the cellular functions are modulated without induction of cell
11 death.^{2,32} Diverse beneficial effects are expected for example in inflammation,³³
12 neurodegenerative diseases,³⁴ muscular dystrophies^{35,36} and cachexia.³⁷ Moreover, they have
13 therapeutic potentialities as antiparasitics in malaria,^{38,39} sleeping syndrome,⁴⁰⁻⁴² and anti-
14 microbial agents (tuberculosis).⁴³ The selective inhibition of immunoproteasomes predominantly
15 expressed in immune cells appears to be a promising rationale for the treatment of autoimmune
16 disorders.³²

17
18
19
20
21
22
23
24
25
26
27
28
29
30
31
32
33
34
35
36
37 The constitutive 26S proteasome contains a barrel-shaped 20S catalytic particle composed of
38 28 subunits capped on either end by a regulatory particle called 19S. The complete subunit
39 architecture of the yeast regulatory 19S particle has been recently described providing insight into
40 recognition and processing of polyubiquitinated substrates.⁴⁴ The architecture of constitutive
41 eukaryotic 20S proteasomes was reported several years ago^{45, 46} and recently compared to that of
42 immunoproteasome.⁴⁷ The 28 subunits (α and β) are arranged in four stacked rings ($\alpha_{1-7}\beta_{1-7}\beta_{1-7}\alpha_{1-7}$)
43 with a 2-fold axial symmetry (Figure 1B).⁴⁵ Three distinct types of catalytic activities are
44 assigned in constitutive proteasomes to two β 1 subunits (caspase-like or post-acid activity, PA),
45 two β 2 subunits (trypsin-like activity, T-L), and two β 5 subunits (chymotrypsin-like activity,
46
47
48
49
50
51
52
53
54
55
56
57
58
59
60

1
2
3 ChT-L). Immunoproteasomes are generated by replacing $\beta 1$, $\beta 2$ and $\beta 5$ subunits by their
4 immuno-homologues $\beta 1i$, $\beta 2i$, and $\beta 5i$ whose synthesis is induced by IFN- γ .^{48, 49}
5
6
7

8 Targeting the ChT-L active site has long been considered as sufficient to develop drugs,
9 especially anti-cancer ones. Nevertheless, inhibition of multiple active sites is required to
10 markedly decrease protein degradation.⁵⁰ Recent data suggest that for anti-cancer drugs it is also
11 important to target the PA in addition to the ChT-L active site.^{51, 52} Moreover, inhibitors of T-L
12 activity sensitize multiple myeloma cells to inhibitors of the ChT-L active site.⁵³ Proteasome
13 inhibitors targeting the T-L activity also appear as the rational choice for anti-trypanosomal drug
14 development.⁵⁴
15
16
17
18
19
20
21
22
23
24

25 Consequently, we developed new noncovalent proteasome inhibitors presenting within the
26 same molecule the possibility to inhibit several active sites. The proteasome catalytic particle
27 presents symmetry related multiple catalytic sites. Thus, chemically symmetrical drugs involving
28 identical inhibitory heads are of significance to provide enhanced inhibitory power. The
29 application of the principle of multivalency has been applied to design potent multivalent
30 inhibitors.⁵⁵ Its application was successful in the protease field⁵⁶ and reported for covalent
31 proteasome inhibitors^{57, 58} and noncovalent ones.⁵⁹ In both cases, two ligands were chemically
32 connected by a PEG spacer to target two active sites in proteasomes. But polydispersity is one of
33 the drawbacks of pegylation,⁵⁹ and access to monodisperse PEG is a challenge.⁶⁰ Here, we
34 describe the design, synthesis and inhibitory efficacies of dimers **4** (Figure 1C) formed of two
35 inhibitory heads derived from the noncovalent proteasome inhibitors **2**, linked by spacers of
36 controlled length to optimally target two selected active sites (Figure 1B). In order to mimic the
37 unfolded protein chain of proteasome substrates that enter the catalytic core, oligomers of amino
38 hexanoic acid (Ahx) and adipic acid derived from **5** or **6** (Figure 1D) were chosen as the spacers.
39
40
41
42
43
44
45
46
47
48
49
50
51
52
53
54
55
56
57
58
59
60

1
2
3 The different moieties constituting the bivalent molecules **4** such as inhibitors **2**, conjugated
4 monomers **3**, and poly Ahx derivatives **5** and **6**, were evaluated independently. The crystal
5 structures of several inhibitors in complex with yeast 20S proteasome were obtained and the
6 mechanism of inhibition determined. Furthermore, the selectivity of action towards challenging
7 proteases such as calpain I and cathepsin B is examined.
8
9

15 RESULTS

17 **Design and Synthesis of Inhibitors.** The design of the bivalent inhibitors relied on the X-ray
18 structure of the yeast 20S proteasome from which distances between the catalytic Thr1O^γ of the
19 different active sites have been determined (Figure 1B).^{45, 61} The two chosen identical inhibitory
20 heads were the tripeptidic sequence found in the noncovalent inhibitors **2a** and **2b** that are linear
21 mimics of the natural product **1** (Figure 1A, C). Their binding to the ChT-L active site of the
22 yeast 20S proteasome was previously characterized by crystallography as well as by their
23 inhibitory potency (IC₅₀ of 1.5 μM and 9.4 μM for **2a** and **2b**, respectively).²³ Compounds **2a** and
24 **2b** displayed identical antiparallel β sheet binding to the S4-S3-S2-S1 proteasomal specificity
25 pocket of the ChT-L active site (Figure S1 in Supporting Information). The C-terminal benzyl
26 group was inserted into the S1 pocket. The reduced activity of the N-terminal deprotected peptide
27 **2b** compared to its Boc analog **2a** was attributed to the disruption of the interaction between β6
28 His98 and the Boc protecting group. So as a bulky lipophilic R group is favorable, we chose to
29 replace the R substituent in **1** by derivatives of Ahx trimer **5a** or tetramer **5b** to generate the new
30 monovalent molecules **3a** and **3b** that could be considered as reference compounds to study the
31 influence of the poly Ahx on the activity of the inhibitory head (Figure 1C, D). Then we built
32 dimers **4** by linking two identical moieties **2b** to oligomers of Ahx (p+q varying from 3 to 8) and
33 adipic acid, in order to simultaneously target two active sites. As the length of extended Ahx and
34
35
36
37
38
39
40
41
42
43
44
45
46
47
48
49
50
51
52
53
54
55
56
57
58
59
60

1
2
3 adipoyl units can be evaluated to *ca.* 10 Å,⁶² the maximum distance between the two *N*-terminus
4 tripeptide nitrogens of dimers **4a-e** may vary discontinuously from 40 to 90 Å (Figure 1C, Tables
5 S1 and S2 in Supporting Information). The lengths of the different spacers are in principle
6 sufficient to potentially bind simultaneously two distinct active sites (distance between two
7 catalytic Thr10^γ from 30 to 65 Å, Figure 1B, C). The diprotected spacers **5** and **6** were prepared
8 from aminohexanoic acid and methyl adipoyl chloride using stepwise conventional peptide
9 synthesis techniques (see scheme for their synthesis in Figure S3, Supporting Information).
10 Saponification of diprotected spacer **5** followed by coupling to tripeptide **2b**²³ afforded reference
11 monovalent compounds **3** in 34-55% overall yield (Scheme 1). Two ways were used to obtain
12 dimers **4**. The first one started from diprotected spacer **6a-c** and **2b**²³ and led to **4a-c** in 22-44%
13 yield. Boc deprotection of monovalent compounds **3** and subsequent coupling to 0.5 equivalent of
14 adipoyl dichloride yielded **4d-e** (25-28%). Target compounds **3** and **4** were characterized by
15 NMR, high resolution mass spectrometry and HPLC.
16
17
18
19
20
21
22
23
24
25
26
27
28
29
30
31
32
33

34 ***In vitro* inhibitory efficiency and mechanism.** We estimated the capacity of compounds **2a-b**,
35 **3a-b**, and **4a-e** to inhibit the ChT-L activity of constitutive human 20S proteasome (fluorogenic
36 substrate Suc-LLVY-AMC), its PA (Z-LLE-β-NA), and its T-L activities (Boc-LRR-AMC) by
37 determining the corresponding IC₅₀ values (Figure S2 in Supporting Information, Table 1).
38 Conversely, no inhibition was observed with poly Ahx derivatives **5d** and **6a**. The deprotection of
39 the *N*-terminal end of the tyrosine residue (R = H, **2b**) compared to **2a** (R = Boc) resulted in an
40 increase of the IC₅₀ value by a factor of 3.6 (ChT-L activity) and 4.4 (PA activity) whereas the T-
41 L activity was abolished. The replacement of the Boc group in **2a** by the longer chains Boc(Ahx)_n
42 (n = 3 for **3a** and 4 for **b**) increased noticeably the inhibitory potency towards the three types of
43 activity: the IC₅₀ values for **3a** were 7-, 2- and 8-times smaller than the IC₅₀ values for the
44 activity: the IC₅₀ values for **3a** were 7-, 2- and 8-times smaller than the IC₅₀ values for the
45
46
47
48
49
50
51
52
53
54
55
56
57
58
59
60

reference **2a** (ChT-L, PA and T-L activities, respectively). These values were more significantly decreased for dimeric inhibitors **4a-e** with factors of 123-167 (ChT-L activity), 19-34 (PA activity), and 355-577 (T-L activity) (compared with **2a**), respectively.

To elucidate the mechanism of inhibition of the ChT-L activity by dimeric inhibitors **4** compared to conjugated monomers **3** and starting molecules **2a-b**, kinetic studies were conducted at a fixed enzyme concentration and various substrate (Suc-LLVY-AMC) and inhibitor concentrations. The tested compounds fall into distinct classes of inhibitors when analyzed by Lineweaver-Burk plots (Figure 2): mixed (**2a**, **3a-b**), non competitive (**2b**) and competitive (**4a-e**). For mixed and non competitive inhibitors, the inhibitors bind to the free (E) and bound enzyme (ES), respectively: $E + I \rightleftharpoons EI$ (inhibitor constant K_i) and $ES + I \rightleftharpoons ESI$ (inhibitor constant K'_i) with $K_i = [E][I]/[EI]$ and $K'_i = [ES][I]/[ESI]$. For competitive inhibitors, they bind only to the free enzyme. *N*-terminal Boc (**2a**) instead of H (**2b**) increased binding into the ChT-L active site (factor of 10 for K_i and 4.8 for K'_i). In the presence of a long Boc(Ahx)_n chain (n = 3 for **3a** and n = 4 for **3b**) instead of Boc (**2a**), the binding to the free enzyme was increased by a factor of 24 and 42, respectively. The binding to the ES complex was also favored (factors of 16-25). These results clearly highlighted the favorable role of the Boc(Ahx)_n chain for inhibitor efficacy, as observed with the natural products fellutamide B,⁶³ glidobactin A⁶⁴ and cepafungin I⁶⁵ which all harbor an aliphatic tail that improves the ligand's affinity to the proteasome. Remarkably, the introduction of a second inhibitory head yielding compounds **4a-e** led to competitive inhibition (Figure 2). The dimeric molecules (**4a-e**) were significantly more potent on the ChT-L activity than **2a** and **2b** with $K_i = 6$ nM for **4e** and $K_i = 10.3-11.4$ nM for **4a-d** whereas $K_i = 2,430$ nM and $K'_i = 5,030$ nM for **2a** and $K_i = K'_i = 24,500$ nM for **2b**, respectively. The ratio of free energies of interaction for the bivalent and monovalent binding ($\beta = K_i^{bi}/K_i^{mono}$)

1
2
3 is large (4,083 for **4e** compared to **2b**), indicating that the binding of the bivalent ligand is
4
5 entropically favored.⁵⁶ Interestingly, the Dixon graphs established for **2a** and **3a** appeared to be
6
7 non linear, but it was linear for the bivalent compound **4b**. The shape of the plots obtained for **2a**
8
9 and **3a** suggested parabolic inhibition in which two molecules of inhibitor are bound per
10
11 molecule of enzyme.⁶⁶ In contrast, only one molecule was susceptible to bind when two
12
13 inhibitory heads are covalently linked within the bivalent inhibitor **4b** in agreement with linear
14
15 Dixon plots.
16
17

18
19 **Structural basis of inhibition.** The crystal structures of 20S yeast proteasome complexed with
20
21 **3a**, **4a** and **4e** were determined at 2.9, 3.1 and 2.8 Å with an $R_{\text{free}} = 22.7\%$, 22.3% and 24.1%,
22
23 respectively (Table 3S, Supporting Information). Well defined electron density maps were
24
25 obtained for all three compounds bound to the ChT-L active site; compound **3a** was also seen in
26
27 the T-L active site. The tripeptide scaffold revealed low Debye-Waller factors indicating a high
28
29 occupancy. As depicted in Figure 3, the inhibitors bound to the ChT-L active site exhibited an
30
31 identical positioning of the tripeptide scaffold with an extended conformation and maintaining
32
33 each amino acid side chain in the same binding pockets as for the original **2a** ligand (Figure S1 in
34
35 Supporting Information). However, as observed for the PEG linkers used in covalent dimerized
36
37 inhibitors,⁵⁷ the poly Ahx linkers of these three compounds were only partially defined due to
38
39 their flexible nature.
40
41
42
43
44

45
46 The superimposition of **2a**, **3a** and **4e** showed no concerted movement of any of the side chains
47
48 in the active site and the respective inhibitors. However, the complex structure of the yeast
49
50 proteasome with **4a** displays a concerted movement of Try96 and His98, thus generating by its
51
52 spacious S4 pocket appropriate space for the linker chain.
53
54

55
56 These results prove that it is predominantly the bivalency of this set of inhibitors which gives
57
58 rise to the high binding preference, though all linkers are defined in the electron density map only
59
60

1
2
3 to the first nitrogen atom. Hence, the analysis of the crystal structure complexes demonstrates
4 multiple conformations for the linker, reiterating the flexibility of the spacer elements. Moreover,
5 a MES molecule was observed in all three structures occupying the oxyanion hole Gly47NH and
6 performing Van der Waals interactions with the inhibitors. Notably, there is 48 Å distance
7 between the two Tyr NH^α of **3a** bound to the β5/β5'subunits, 54 Å for β2/β2', 47 Å for intra-ring
8 β5/β2, and 25 Å for inter-ring β5/β2', thus allowing simultaneous binding of the bivalent
9 inhibitors to two different active sites, explaining the low IC₅₀ values.
10
11
12
13
14
15
16
17
18
19

20 **Effect of bivalent inhibitors in human cells.** We treated HEK-293 cells with the various
21 compounds for 2 h and determined their proteasome inhibition profile (Figure 4, Table 2).
22 Monovalent **3a** and bivalent molecules (**4a-e**) inhibited the ChT-L activity at submicromolar
23 concentrations (IC₅₀ of 252-756 nM). Much higher concentrations of the parent molecule **2a** were
24 required (IC₅₀ = 7.97 μM). The PA activity was poorly inhibited (IC₅₀ of about 20 μM). The
25 reference molecule epoxomicin appeared to be a stronger inhibitor of both ChT-L ad PA
26 activities but only by a factor of 18 (ChT-L activity) and 15 (PA activity) when exemplarily
27 compared to **4c**.
28
29
30
31
32
33
34
35
36
37
38

39 **Specificity and metabolic stability.** All synthesized compounds were analyzed for their effect
40 on two representative cellular proteases, cytosolic calpain I and lysosomal cathepsin B. No
41 significant inhibition was observed at 20 μM. Furthermore, the stability of compounds **2a**, **3a** and
42 **4a** in the biological medium used in cellular studies was determined in order to evaluate their
43 susceptibility to enzymatic hydrolysis. They were incubated at 37°C in the culture medium
44 (RPMI) in the presence of 20% fetal calf serum for different periods of time. Kinetics were
45 followed by HPLC. The HPLC results showed that the peak area of compounds **2a** and the
46
47
48
49
50
51
52
53
54
55
56
57
58
59
60

1
2
3 bivalent inhibitor **4a** did not change or deviate over time, indicating stability within 50 h
4
5 compared to the monovalent compound **3a** (degradation half-time of 19 h).
6
7

8 DISCUSSION

9
10 The principle of polyvalency is ubiquitously exploited in nature.^{55,56} It led medicinal chemists
11
12 to take advantage of multivalent binding to design new molecules with increased binding affinity
13
14 and selectivity. This alternative approach is particularly pertinent for the multicatalytic 20S
15
16 proteasome and has been used to generate homo- and heterobivalent proteasome covalent
17
18 binders.^{57,58} Homodimers of tripeptidic aldehydes linked by a polydisperse PEG spacer led to
19
20 efficient covalent inhibitors of ChT-L activity which potency was increased 123-fold.⁵⁷ Here we
21
22 present homobivalent molecules formed by two noncovalent inhibitory heads linked by a
23
24 monodisperse poly Ahx spacer.
25
26
27

28
29 Inspection of the *in vitro* inhibition data in conjunction with the crystallographic data revealed
30
31 interesting features of the new bivalent inhibitors. Compared to the reference molecule **2a**, the
32
33 dimeric inhibitors **4a-e** displayed efficacies noticeably increased by factors of 133-167 (ChT-L
34
35 activity), 19-34 (PA activity) and 355-577 (T-L activity). Out of the substances prepared, five
36
37 show inhibitory activity against human proteasome ChT-L site comparable to the parent cyclic
38
39 molecule **1**: K_i of 6.0-11.4 nM for **4a-e** in the range of that obtained by **1** ($K_i = 2.3$ of nM).
40
41 Remarkably, the T-L activity was more efficiently blocked by the bivalent molecules than by **1**
42
43 (factors of 10-16 between the IC_{50} values). Smaller differences were observed for the PA activity
44
45 (6-10). Importantly, the mechanism of inhibition of the ChT-L activity is shifted from mixed for
46
47 the starting linear mimics **2a** and poly Ahx monomers **3a-b** to competitive inhibition for the
48
49 bivalent compounds **4a-e**. This highlights on the one hand the influence on the mechanism of the
50
51 substituent at the *N*-terminal end of the peptide, and on the other hand, the importance of the
52
53 presence of a second inhibitory head. The influence of a (Ahx)₃ *N*-terminal extension on both
54
55
56
57
58
59
60

1
2
3 efficiency and selectivity of proteasome inhibitors was previously noticed for covalent peptide
4 vinyl sulfones.⁶⁷ Finally, the reference starting molecule (**2a**), monovalent (**3a**) and bivalent (**4a**)
5
6
7
8 compounds showed a promising stability in cell culture medium with half-lives of over 60 h (**2a**
9
10 and **4a**) and 19 h (**3a**), respectively.

11
12 The proteasome is a valid drug target for cancer but also for sleeping sickness.^{40,41} It was
13 demonstrated that the proteasome from *Trypanosoma brucei* is particularly sensitive to inhibition
14
15 of its T-L activity.^{54,68,69} Recent research has shown that T-L activities of trypanosome and
16
17
18 mammalian proteasomes may have distinct sensitivities for inhibitors.⁷⁰ Nevertheless, it is
19
20 reasonable to assume that bivalent inhibitors targeting simultaneously T-L and ChT-L activities
21
22 of mammalian proteasomes may provide a new opportunity for the development of drugs to be
23
24
25 implemented in treating sleeping sickness disease.
26
27

28 29 CONCLUSION

30
31 Proteasome inhibitors have a vast therapeutic potential, but resistance and poor efficacy of
32
33 clinical covalent inhibitors on some solid tumors demonstrate the need for molecules with a new
34
35 mechanism of action. We pursue a noncovalent strategy with inhibitors theoretically free from
36
37 the inherent drawbacks associated to the presence of a reactive group by designing dimerized
38
39 linear mimics of **1**. To optimally target two selected active sites, monodisperse poly Ahx spacers
40
41 were used to avoid the polydispersity of PEG spacers or detergent-like properties of compounds
42
43 with long alkyl chains. We have generated a new set of dimerized noncovalent inhibitors for
44
45 which blockage of the proteasome *in vitro* or in cellular assays is strongly enhanced. Their
46
47 mechanism of action is corroborated by crystallographic studies. Crossing simple chemistry and
48
49 taking advantage of the proteasome C_2 -symmetry lead to inhibitor activity similar to the reference
50
51 natural product **1**. Remarkably the specificity of inhibition was significantly improved by the
52
53 synthesized bivalent ligands. Thus, the presented results open new possibilities for efficient and
54
55
56
57
58
59
60

1
2
3 controlled inhibition of two types of active sites using a single probe. Synergistic effects to
4
5 decrease protein degradation may be induced favoring the inhibitor action in several pathologies.
6
7
8
9
10
11
12
13
14
15
16
17
18
19
20
21
22
23
24
25
26
27
28
29
30
31
32
33
34
35
36
37
38
39
40
41
42
43
44
45
46
47
48
49
50
51
52
53
54
55
56
57
58
59
60

EXPERIMENTAL SECTION

Chemistry. Commercially available reagents were used without further purification unless otherwise stated. Dry solvents were distilled from the appropriate drying reagents immediately before use. Yields refer to chromatographically and spectroscopically homogeneous materials, unless otherwise stated. Reactions were monitored by thin-layer chromatography carried out on silica gel aluminium sheets (60F-254) using UV light as a visualizing agent, 15% ethanolic phosphomolybdic acid and heat or 0.2% ethanolic ninhydrin and heat as developing agent. Column chromatography was performed on silica gel 60, 0.063-0.200 mm. MPLC (medium pressure liquid chromatography) was performed on a Flashsmart two apparatus, using C18 silica flash column (prepacked column, 4.3g C18 silica, AIT chromato, 40 -60 μm). ^1H NMR and ^{13}C NMR spectra were recorded at room temperature on a BRUCKER Avance 300 or Avance 500 spectrometers. Chemical shifts were reported in ppm (δ units) and residual non deuterated solvent was used as internal reference. High-resolution mass spectra were recorded on a Waters Q-TOF 2 or a Bruker Micro-TOF Q II apparatus using an electrospray source (ESI). Melting points were measured on a Stuart melting point apparatus. Microanalysis and mass spectra were performed by the Centre régional des mesures physiques de l'Ouest (CRMPO, Rennes, France). Anhydrous hydrogen chloride 3.3 M in anhydrous methanol was generated by reaction of acetyl chloride (2.34 mL, 33 mmol) with anhydrous methanol (10 mL). Tripeptides **2a-b** were previously described.²³ Amino hexanoic acid derivatives HCl, H-Ahx-OMe,⁷¹ Boc-Ahx-OH⁷² and Boc-Ahx-OSu⁷³ were prepared according known procedures. Scheme for the synthesis of compounds **3-6** is given in Supporting Information (Figure S3). Purity of building blocks **5a-e** and **6a-c** was checked by elemental analysis. Data for C, H, and N were within 0.4% of the theoretical values. Purity of compounds **3-4**, was determined by reverse phase HPLC using a C18 column (5 μm , 4.6

1
2
3 mm X 250 mm, ACE), detection at 254 nm, a 1 mL per minute flow rate and solvent A (50:50
4 MeOH/water) for 2 min then a linear gradient from 100% of solvent to 100% of solvent B (85:15
5 MeOH/water) for 20 min then solvent B for 16 min. Purity was higher than 95% for all
6
7
8
9
10
11 compounds except for compounds **4c** (88 %) and **4d** (78%).

12
13 *Monovalent inhibitor 3a*: Tripeptide hydrochloride **2b** (135 mg, 0.197 mmol) was
14 dissolved in water (4 mL) and treated with aqueous 4 M NaOH (1 mL). The aqueous solution
15 was extracted three times by ethyl acetate. The combined organic phases were dried over sodium
16 sulfate and concentrated *in vacuo* to afford basic tripeptide **2b** (121,1 mg, 0.186 mmol). A
17 solution of Boc-(Ahx)₃-OH (obtained from 0.154 mmol Boc-(Ahx)₃-OMe **5a**) in anhydrous DMF
18 (1 mL) was reacted under Ar overnight at room temperature with HOBt (26.10 mg, 0.17 mmol),
19 EDC, HCl (32.05 mg, 0.167 mmol), Et₃N (0.026 mL, 0.184 mmol) and a solution of tripeptide **2b**
20 (0.186 mmol) in anhydrous DMF (2 mL). The mixture was concentrated *in vacuo* and the
21 resulting solid was washed by water, 0.1 M hydrochloric acid and then water. After
22 chromatography through silica gel (13 g, eluent 5 % to 10 % MeOH in CH₂Cl₂) compound **3a**
23 (90.84 mg, yield 55 %) was afforded as a white solid. R_f = 0.19 (10 % MeOH in CH₂Cl₂). ¹H
24 NMR (300 MHz, DMSO-d₆) δ 1.04-1.46 (m, 30 H), 2.00 (t, *J* = 7 Hz, 6H), 2.09 (dd, *J* = 14.5 Hz,
25 *J* = 9 Hz, 1H), 2.38 (m, 1H), 2.62 (m, 1H), 2.82-3.00 (m, 7H), 4.04-4.27 (m, 4H), 4.45 (m, 1H),
26 5.02 (s, 2H), 6.01 (s, 1H), 6.75 (d, *J* = 7.5 Hz, 2H), 6.87-6.95 (m, 3H), 7.08-7.43 (m, 18 H), 7.71
27 (m, 2H), 7.76 (d, *J* = 8 Hz, 1H), 7.91-7.98 (m, 2H), 8.08 (d, *J* = 6.5 Hz, 1H), 10.12 (s, 1H).
28
29 HPLC: Rt. 26.1 min, area percent 97% at 254 nm. HRMS (ESI) calcd for C₆₀H₈₀N₈O₁₁Na
30 [(M+Na)⁺] 1111.5844, found 1111.5841.
31
32
33
34
35
36
37
38
39
40
41
42
43
44
45
46
47
48
49
50
51
52

53 *Monovalent inhibitor 3b*: A solution of Boc-(Ahx)₄-OH (115.3 mg, 0.202 mmol, obtained
54 from Boc-(Ahx)₄-OMe **5b**) in anhydrous DMF (2 mL) was reacted overnight under Ar and at
55
56
57
58
59
60

1
2
3 room temperature with HOBt (34 mg, 0.22 mmol), EDC, HCl (42 mg, 0.219 mmol), Et₃N (0.034
4 mL, 0.24 mmol) and basic tripeptide **2b** (0.26 mmol) in anhydrous DMF (2 mL). The mixture
5
6 was concentrated *in vacuo* and the resulting solid was washed by water, 0.1 M hydrochloric acid
7
8 then water. After medium pressure chromatography through C-18 reversed phase silica gel
9
10 (eluent 0.001 M aqueous HCl /MeOH 100/0 to 0/100) compound **3b** (82.4 mg, yield 34 %) was
11
12 afforded as a white solid. R_f = 0.20 (10 % MeOH in CH₂Cl₂). ¹H NMR (500 MHz, CD₃OD) δ
13
14 1.19-1.61 (m, 36H), 2.13-2.25 (m, 8H), 2.46 (dd, *J* = 9.6 Hz, *J* = 14 Hz, 1H), 2.59 (dd, *J* = 3.1
15
16 Hz, *J* = 14 Hz, 1H), 2.78 (dd, *J* = 9.5 Hz, *J* = 14 Hz, 1H), 3.00-3.33 (m, 9H), 4.16 (q, *J* = 7.3 Hz,
17
18 1H), 4.19 (dd, *J* = 2.8 Hz, *J* = 9.5 Hz, 1H), 4.26 and 4.39 (*J*_{AB} = 15.0 Hz, 2H), 4.47 (dd, *J* = 5.2
19
20 Hz, *J* = 9.6 Hz, 1H), 5.06 (s, 2H), 6.85 (d, *J* = 7.0 Hz, 1H), 6.90 (d, *J* = 8.5 Hz, 2H), 7.04 (t, *J* =
21
22 8.0 Hz, 1H), 7.12 (d, *J* = 8.5 Hz, 2H), 7.18-7.42 (m, 12H). ¹³C NMR (125.77 MHz, CD₃OD) δ
23
24 17.2 (CH₃), 23.4 (CH₂), 26.4 (CH₂), 26.6 (CH₂), 26.7 (CH₂), 26.8 (CH₂), 27.4 (CH₂), 27.5 (CH₂),
25
26 27.6 (CH₂), 28.8 (CH₃), 30.0 (CH₂), 30.1 (CH₂), 30.7 (CH₂), 36.6 (CH₂), 37.0 (CH₂), 37.8 (CH₂),
27
28 37.4 (CH₂), 39.7 (CH₂), 40.2 (CH₂), 40.3 (CH₂), 44.1 (CH₂), 51.3 (CH), 51.5 (CH), 56.6 (CH),
29
30 71.0 (CH₂), 76.4 (C), 79.6 (C), 111.4 (CH), 115.9 (CH), 123.9 (CH), 125.5 (CH), 128.1 (CH),
31
32 128.4 (CH), 128.6 (CH), 128.8 (CH), 129.4 (CH), 129.5 (CH), 130.6 (C), 130.9 (CH), 131.3
33
34 (CH), 131.8 (C), 138.8 (C), 139.7 (C), 142.9 (C), 158.5 (C), 159.1(C), 172.2 (C), 173.5 (C),
35
36 174.8 (C), 175.9 (C), 176.0 (C), 176.1 (C), 176.6 (C), 181.5 (C). HPLC: Rt. 25.7 min, area percent
37
38 95% at 254 nm. HRMS (ESI) calcd for C₆₆H₉₁N₉O₁₂Na [(M+Na)⁺] 1224.6685, found 1224.6681.
39
40
41
42
43
44
45
46
47

48
49 *Bivalent inhibitor 4a*: (p+q = 3, p=0) A solution of MeO-Adip-Ahx₃-OMe **6a** (218.8 mg,
50
51 0.426 mmol) in THF (1.5 mL) was reacted for 3.5 h at room temperature with 1 M LiOH (1.5
52
53 mL, 1.5 mmol) and then treated by concentrated HCl. The white precipitate was filtered, washed
54
55 by water, and dried to afford HO-Adip-Ahx₃-OH (154.7 mg, yield 75 %) which was used without
56
57
58
59
60

1
2
3 further purification. A solution of HO-Adip-(Ahx)₃-OH (10.89 mg, 0.0224 mmol) in anhydrous
4 DMF (0.4 mL) was reacted under Ar for 72 h at room temperature with HOBt (7.62 mg, 0.056
5 mmol), EDC, HCl (10.83 mg, 0.0565 mmol), Et₃N (0.008 mL, 0.057 mmol) and basic tripeptide
6 **2b** (39.12 mg, 0.0602 mmol). The mixture was concentrated *in vacuo* and the resulting solid was
7 washed by water, 0.1 M hydrochloric acid and then water. After purification by medium pressure
8 chromatography through C-18 reversed phase silica gel (eluent 0.001 M aqueous HCl /MeOH,
9 gradient from 100/0 to 0/100) dimeric compound **4a** (17.56 mg, yield 44 %) was afforded as a
10 white solid. R_f = 0.40 (15 % MeOH in CH₂Cl₂). ¹H NMR (500 MHz, DMSO-d₆) δ 1.08-1.35 (m,
11 24H), 1.46 (m, 4H), 2.01 (m, 10H), 2.11 (dd, *J* = 9 Hz, *J* = 14.5 Hz, 2H), 2.45 (m, 2H), 2.65 (m,
12 2H), 2.98 (m, 8H), 4.07-4.26 (m, 8H), 4.46 (m, 2H), 5.04 (s, 4H), 6.03 (s, 2H), 6.76 (d, *J* = 7 Hz,
13 2H), 6.89 (d, *J* = 8 Hz, 4H), 6.94 (t, *J* = 8 Hz, 2H), 7.14-7.44 (m, 28H), 7.68 (m, 3H), 7.76 (dd, *J*
14 = 7 Hz, *J* = 1.5 Hz, 2H), 7.93 (t, *J* = 6 Hz, 2H), 7.98 (m, 2H), 8.10 (m, 2H), 10.13 (s, 2H). HPLC:
15 Rt. 27.2 min, area percent > 99% at 254 nm. HRMS (ESI) calcd for C₉₈H₁₁₇N₁₃O₁₇Na [(M+Na)⁺]
16 1770.8588, found 1770.8586.
17
18
19
20
21
22
23
24
25
26
27
28
29
30
31
32
33
34
35

36 *Bivalent inhibitor 4b*: (p+q = 4, p=0) Similarly, a solution of HO-Adip-(Ahx)₄-OH (12.33
37 mg, 0.0206 mmol, prepared from MeO-Adip-(Ahx)₄-OMe **6b**) in anhydrous DMF (0.5 mL) was
38 reacted under Ar for 72 h at room temperature with HOBt (7.74 mg, 0.051 mmol), EDC, HCl
39 (13.37 mg, 0.0697 mmol), Et₃N (0.008 mL, 0.057 mmol) and basic tripeptide **2b** (37.7 mg,
40 0.0581 mmol). The mixture was concentrated *in vacuo* and the resulting solid was washed by
41 water, 0.1 M hydrochloric acid and then water. After purification by medium pressure
42 chromatography through C-18 reversed phase silica gel (eluent 0.001 M aqueous HCl /MeOH,
43 gradient from 100/0 to 0/100) dimeric compound **4b** (15.28 mg, yield 40 %) was afforded as a
44 white solid. ¹H NMR (500 MHz, DMSO-d₆) δ 1.08-1.36 (m, 28H), 1.46 (m, 6H), 2.01 (m, 12H),
45
46
47
48
49
50
51
52
53
54
55
56
57
58
59
60

1
2
3 2.11 (dd, $J = 9$ Hz, $J = 14.5$ Hz, 2H), 2.45 (dd, $J = 4$ Hz, $J = 14.5$ Hz, 2H), 2.65 (m, 2H), 3.00 (m,
4
5 10H), 4.07-4.26 (m, 8H), 4.46 (m, 2H), 5.04 (s, 4H), 6.04 (s, 2H), 6.77 (d, $J = 7$ Hz, 2H), 6.89 (d,
6
7 $J = 8$ Hz, 4H), 6.94 (t, $J = 7.5$ Hz, 2H), 7.14-7.44 (m, 28H), 7.68-7.72 (m, 4H), 7.76 (dd, $J = 9$
8
9 Hz, $J = 4$ Hz, 2H), 7.94 (t, $J = 6$ Hz, 2H), 7.99 (m, 2H), 8.10 (m, 2H), 10.13 (s, 2H). HPLC: Rt.
10
11 27.1 min, area percent 95% at 254 nm. HRMS (ESI) calcd for $C_{104}H_{128}N_{14}O_{18}Na [(M+Na)^+]$
12
13 1883.9429, found 1883.9453.
14
15

16
17 *Bivalent inhibitor 4c*: ($p+q = 5$, $p=0$) Similarly, a solution of HO-Adip-(Ahx)₅-OH (14.56
18
19 mg, 0.0205 mmol, prepared from MeO-Adip-(Ahx)₅-OMe **5c**) in anhydrous DMF (0.5 mL) was
20
21 reacted under Ar for 72 h at room temperature with HOBt (7.29 mg, 0.047 mmol), EDC, HCl
22
23 (20.33 mg, 0.106 mmol), Et₃N (0.008 mL, 0.057 mmol) and basic tripeptide **2b** (37.7 mg, 0.0581
24
25 mmol). The mixture was concentrated *in vacuo* and the resulting solid was washed by water, 0.1
26
27 M hydrochloric acid and then water. After purification by medium pressure chromatography
28
29 through C-18 reversed phase silica gel (eluent 0.001 M aqueous HCl /MeOH, gradient from
30
31 100/0 to 0/100) dimeric compound **4c** (9.02 mg, yield 22 %) was afforded as a white solid. ¹H
32
33 NMR (500 MHz, DMSO-d₆) δ 1.17-1.36 (m, 32H), 1.46 (m, 8H), 2.02 (m, 14H), 2.12 (dd, $J =$
34
35 8.5 Hz, $J = 14$ Hz, 2H), 2.42 (m, 2H), 2.62 (m, 2H), 3.00 (m, 12H), 4.07-4.26 (m, 8H), 4.46 (m,
36
37 2H), 5.04 (s, 4H), 6.04 (br s, 2H), 6.77 (d, $J = 7.5$ Hz, 2H), 6.89 (d, $J = 7$ Hz, 4H), 6.94 (t, $J = 7.5$
38
39 Hz, 2H), 7.14-7.44 (m, 28H), 7.71-7.72 (m, 5H), 7.76 (m, 2H), 7.94 (t, $J = 6$ Hz, 2H), 7.99 (m,
40
41 2H), 8.10 (m, 2H), 10.13 (s, 2H). HPLC: Rt. 26,8 min, area percent 88% at 254 nm. HRMS (ESI)
42
43 calcd for $C_{110}H_{139}N_{15}O_{19}Na [(M+Na)^+]$ 1997.0264, found 1997.0351.
44
45
46
47
48
49

50
51 *Bivalent inhibitor 4d*: ($p+q = 6$, $p = 3$) A solution of **3a** (86.85 mg, 0.0809 mmol) in
52
53 MeOH (2 mL) at 0 °C was reacted for 6 min with 12 M anhydrous HCl in MeOH (1.8 mL, 25
54
55 mmol) and then concentrated *in vacuo* without heating. The resulting solid was dissolved in water
56
57
58
59
60

1
2
3 (3 mL) and reacted with aqueous 4 M NaOH (1 mL). Extraction by ethyl acetate quantitatively
4
5 yielded basic deprotected **3a**. This product was dissolved in anhydrous DMF (0.5 mL) and was
6
7 reacted under Ar with Et₃N (0.008 mL, 0.057 mmol) and adipoyl dichloride (3.2 μL, 0.022
8
9 mmol) for 72 h at room temperature. The mixture was concentrated *in vacuo* and the resulting
10
11 solid was purified by medium pressure chromatography through C-18 reversed phase silica gel
12
13 (eluent 0.001 M aqueous HCl /MeOH, gradient from 100/0 to 0/100). Dimeric compound **4d**
14
15 (12.9 mg, yield 28 %) was afforded as a white solid. ¹H NMR (500 MHz, DMSO-d₆) δ 1.09-1.36
16
17 (m, 36H), 1.44 (m, 10H), 2.02 (m, 16H), 2.11 (dd, *J* = 9 Hz, *J* = 14 Hz, 2H), 2.45 (m, 2H), 2.64
18
19 (m, 2H), 3.00 (m, 14H), 4.09-4.23 (m, 8H), 4.47 (m, 2H), 5.04 (s, 4H), 6.03 (s, 2H), 6.77 (d, *J* =
20
21 7.5 Hz, 2H), 6.89 (d, *J* = 7 Hz, 4H), 6.94 (t, *J* = 7.5 Hz, 2H), 7.14-7.44 (m, 28H), 7.71-7.72 (m,
22
23 6H), 7.77 (d, *J* = 7.5 Hz, 2H), 7.94 (t, *J* = 6 Hz, 2H), 7.98 (d, *J* = 8 Hz, 2H), 8.10 (d, *J* = 7 Hz,
24
25 2H), 10.13 (s, 2H). HPLC: Rt. 26,3 min, area percent 78% at 254 nm. HRMS (ESI) calcd for
26
27 C₁₁₆H₁₅₀N₁₆O₂₀Na [(M+Na)⁺] 2110.1100, found 2110.1130.
28
29
30
31
32
33

34 *Bivalent inhibitor 4e*: (p+q = 8, p = 4) A solution of **3b** (66 mg, 0.055 mmol) in MeOH (2
35
36 mL) at 0 °C was reacted for 6 min with 12 M anhydrous HCl in MeOH (0.26 mL, 3.1 mmol) and
37
38 then concentrated *in vacuo* without heating. The resulting solid was dissolved in anhydrous DMF
39
40 (0.34 mL) and was reacted under Ar with Et₃N (0.052 mL, 0.358 mmol) and adipoyl dichloride
41
42 (5.0 μL, 0.033 mmol) for 72 h at room temperature. The mixture was concentrated *in vacuo* and
43
44 the resulting solid was purified by medium pressure chromatography through C-18 reversed
45
46 phase silica gel (eluent 0.001 M aqueous HCl /MeOH, gradient from 100/0 to 0/100) followed by
47
48 a second purification (eluent water/MeOH, gradient from 50/50 to 0/100, fraction analysis by
49
50 HPLC). Dimeric compound **4e** (16 mg, yield 25 %) was afforded as a white solid after
51
52 lyophilisation. ¹H NMR (500 MHz, CD₃OD) δ 1.19-1.65 (m, 58H), 2.19-2.25 (m, 20H), 2.48 (dd,
53
54
55
56
57
58
59
60

1
2
3 $J = 9.5$ Hz, $J = 14$ Hz, 2H), 2.61 (dd, $J = 3.1$ Hz, $J = 14$ Hz, 2H), 2.80 (dd, $J = 9.5$ Hz, $J = 14$ Hz,
4 2H), 3.09 (dd, $J = 5$ Hz, $J = 14$ Hz, 2H), 3.14-3.21 (m, 16H), 4.16 (q, $J = 7.5$ Hz, 2H), 4.21 (dd, J
5 = 3 Hz, $J = 9.5$ Hz, 2H), 4.28 and 4.41 ($J_{AB} = 15.5$ Hz, 4H), 4.48 (dd, $J = 5.5$ Hz, $J = 9.5$ Hz, 2H),
6 5.06 (s, 4H), 6.87 (d, $J = 7.5$ Hz, 2H), 6.92 (d, $J = 8.5$ Hz, 4H), 7.06 (t, $J = 8.0$ Hz, 2H), 7.14 (d, J
7 = 8.5 Hz, 4H), 7.19-7.44 (m, 24H). ^{13}C NMR (125.77 MHz, CD_3OD) δ 17.2 (CH_3), 26.3 (CH_2),
8 26.4 (CH_2), 26.6 (CH_2), 26.7 (CH_2), 27.4 (CH_2), 27.5 (CH_2), 27.6 (CH_2), 30.0 (CH_2), 36.5 (CH_2),
9 36.6 (CH_2), 36.7 (CH_2), 37.4 (CH_2), 39.7 (CH_2), 40.3 (CH_2), 40.4 (CH_2), 40.5 (CH_2), 44.1 (CH_2),
10 51.4 (CH), 51.6 (CH), 56.7 (CH), 71.0 (CH_2), 76.4 (C), 111.4 (CH), 115.9 (CH), 123.9 (CH),
11 125.5 (CH), 128.1 (CH), 128.4 (CH), 128.6 (CH), 128.8 (CH), 129.4 (CH), 129.5 (CH), 130.6
12 (C), 130.9 (CH), 131.3 (CH), 131.8 (C), 138.8 (C), 139.7 (C), 142.9 (C), 159.1 (C), 173.2 (C),
13 174.5 (C), 174.8 (C), 176.0 (C), 176.3 (C), 176.4 (C), 176.6 (C), 181.5 (C). HPLC: Rt. 27.4 min,
14 area percent 96% at 254 nm. HRMS (ESI) calcd for $\text{C}_{128}\text{H}_{172}\text{N}_{18}\text{O}_{22}\text{Na}$ [(M+Na) $^+$] 2336.2791,
15 found 2336.2758.
16
17
18
19
20
21
22
23
24
25
26
27
28
29
30
31
32
33

34 **Enzyme activity and inhibition assays using purified enzymes.** Purified human constitutive
35 20S proteasome from erythrocyte was obtained from Boston Biochem (Euromedex, France). All
36 substrates (Suc-LLVY-AMC, Boc-LRR-AMC and Z-LLE-BNA) were obtained from Bachem
37 (Weil am Rhein, Germany).
38
39
40
41
42

43 Proteasome activities were determined *in vitro* by monitoring the hydrolysis of the $\beta 5$ (ChT-L)
44 substrate Suc-LLVY-AMC, $\beta 1$ (PA) substrate Z-LLE- β NA, and $\beta 2$ (T-L) substrate Boc-LRR-
45 AMC for 45 min 37°C in the presence of untreated proteasome (control) or proteasome that had
46 been previously incubated during 15 min in the presence of the applied compound at the chosen
47 concentration. The excitation wavelengths were 360 nm (AMC substrates) and 340 nm (β NA
48 substrate) whereas the emission wavelengths were 460 nm (AMC substrates) and 405 nm (β NA
49 substrate).
50
51
52
53
54
55
56
57
58
59
60

substrate), respectively. Substrate and compounds were previously dissolved in DMSO. The final DMSO concentration was kept constant at 2% (v/v) in all assays. Buffers were composed of 20 mM Tris (pH 7.5), 10% (v/v) glycerol, 0.01% (w/v) SDS (ChT-L and PA activities); 20 mM Tris (pH 8.0), 10% (v/v) glycerol, 0.01% (w/v) for T-L activity. The final enzyme concentrations were 0.3 nM (20S proteasome) using 20 μM Suc-LLVY-AMC (ChT-L), 50 μM Z-LLE-βNA (PA) and 20 μM Boc-LRR-AMC (T-L). Initial rates determined in control experiments (V_0) were considered to be 100% of the peptidase activity while initial rates below 100% were considered to be inhibitions. The values of IC_{50} (compound concentrations resulting in 50% enzyme inhibition) were calculated by fitting the experimental data to the equation 1 or equation 2.

$$\%inhibition = 100 \times (1 - V_i/V_0) = \frac{100 \times IC_{50}}{IC_{50} + [I]_0} \quad (\text{eq. 1})$$

$$\%inhibition = \frac{100 \times [I]_0^{nH}}{IC_{50}^{nH} + [I]_0^{nH}} \quad (\text{eq. 2})$$

Reaction rates determined at fixed enzyme concentration and varying substrate and inhibitor concentrations were fitted by non-linear regression to the following Michaelis-Menten-type equations; equation 3 for competitive and equation 4 for non competitive ($K_i = K'_i$) and mixed inhibitions ($K_i \neq K'_i$):

$$V_i = \frac{V_{\max} \times [S]_0}{[S]_0 + K_m(1 + [I]/K_i)} \quad (\text{eq. 3})$$

$$V_i = \frac{V_{\max} \times [S]_0}{[S]_0 + \frac{K_m(1 + [I]/K'_i)}{(1 + [I]/K_i)}} \quad (\text{eq. 4})$$

with K_m , Michaelis constant; V_{\max} , maximum initial rate; K_i , dissociation constant of EI; K'_i , dissociation constant of ESI. Lineweaver-Burk ($1/V_i = f(1/[S]_0)$) and Eadie-Hostee ($V_i = f(V_i/[S]_0)$) representations were also used in routine to conveniently visualize the mechanism of proteasomal blockage and determine the corresponding kinetic constants K_i or K'_i . Dixon graphs ($V_0/V_i = f([I])$) were also constructed.

The activity of human calpain I in the absence and in the presence of a tested compound was determined by monitoring the hydrolysis of the fluorogenic substrate Suc-LLVY-AMC (50 μM) for 30 min in 50 mM Tris HCl, 2 mM CaCl_2 , 10 mM DTT ($[E]_0 = 81 \text{ nM}$; ($\lambda_{\text{exc}} = 360 \text{ nm}$ and $\lambda_{\text{em}} = 460 \text{ nm}$; pH 7.2; 25°C). Human cathepsin B activity ($[E]_0 = 0.55 \text{ nM}$) was received by monitoring the hydrolysis of the fluorogenic substrate Z-RR-AMC (50 μM ; $\lambda_{\text{exc}} = 360 \text{ nm}$, $\lambda_{\text{em}} = 460 \text{ nm}$) for 30 min at 37°C in the presence of untreated proteasome (control) or proteasome that had been incubated for 5 min with the appropriate compound. The buffer was: 352 mM KH_2PO_4 , 48 mM Na_2HPO_4 , 1 mM EDTA, 1 mM DTT (pH 6.0). Substrate was previously dissolved in water and all compounds in DMSO. Calpain I (or cathepsin B) and the respective inhibitor were incubated for 5 min (or 15 min) before the measurement of the remaining enzyme activity. The IC_{50} values were obtained by adjusting the experimental points to eq 1 or 2.

Cell-based Proteasome-Glo™ $\beta 1$, $\beta 2$, and $\beta 5$ assay. The effects of the compounds on ChT-L, PA and T-L activities of HEK-293 cells were determined using a chemiluminescent assay (Proteasome Glo Cell-Based Assay, Promega). HEK-293 cells were dispensed into white opaque 384-well microtiter plates (2,500 cells/well, 50 μL culture medium per well). 0.5 μL of each

1
2
3 compound previously dissolved in DMSO was added. An equivalent volume of DMSO was used
4
5 in controls for a final DMSO concentration of 1% (v/v). After an incubation period of 2 h, 25 μ L
6
7 assay buffer containing a recombinant firefly luciferase and the luminogenic proteasome
8
9 substrate Suc-LLVY-GloTM (ChT-L activity), Z-nLPnLD-GloTM (PA activity) or Z-LRR-GloTM
10
11 (T-L activity) was added. After a further incubation at room temperature for 10 min,
12
13 chemiluminescence expressed as RLU (Relative Light Units), was measured on a BMG Labtech
14
15 Fluostar optima plate reader with a measuring time of 12 s for each well. The final concentrations
16
17 of tested compounds varied between 2 - 20 μ M.
18
19

20
21
22 Remaining ChT-L, PA or T-L activities were determined according to equation 5:
23

24
25
26
27
28

$$\%Activity = 100 \times \left(1 - \frac{Activity_i}{Activity_0} \right) = 100 - \left(\frac{100 \times [I]_0^n}{IC_{50}^n + [I]_0^n} \right) \quad (\text{eq. 5})$$

29
30
31 **Stability.** Stock solutions of compounds dissolved in DMSO were prepared (5 mM) and
32
33 diluted in the biological medium RPMI containing 20% fetal serum. The final concentration of
34
35 each sample was 50 μ M with 1% DMSO. These samples were left in an incubator at 37°C for 47
36
37 h. Aliquots were withdrawn at various times (0, 17, 23, 41 and 47 h); proteins were precipitated
38
39 by ethanol (final concentration 20%). After centrifugation (10,000 rpm, 10 min), the supernatant
40
41 was analyzed by HPLC (C18-reverse phase column, 5 μ m, 4.6 mm x 250 mm, isocratic
42
43 60/40/0.1 CH₃CN/H₂O/TFA, 1 mL per min, detection at 254 nm) to determine the amount of the
44
45 respective compound present in each aliquot at 0, 17, 23, 41 and 47 hours. Finally, peak areas
46
47 were plotted against the time.
48

49
50 **Crystallization and structure determination.** Crystals of the 20S proteasome from *S.*
51
52 *Cerevisiae* were grown in hanging drops at 24 °C as previously described^{74,75} and incubated for at
53
54 least 48 h with their respective **1** derivatives. 40 mg/mL protein concentration was used for
55
56 crystallization in Tris-HCl (10 mM, pH 7.5) and EDTA (1 mM). The drops contained 3 μ L of
57
58
59
60

1
2
3 protein and 2 μL of the reservoir solution, consisting of 30 mM of Magnesium Acetate (MgAc_2),
4
5 100 mM of morpholino-ethane-sulphonic acid (MES) (pH 6.8) and 10% of 2-methyl-2,4-
6
7 pentandiol (MPD). Crystals were soaked in a cryoprotecting buffer (30% MPD, 20 mM MgAc_2 ,
8
9 100 mM MES pH 6.8), frozen in a stream of liquid nitrogen gas at 100 K (Oxford Cryo Systems)
10
11 for data collection. The space group of CP: **1** derivative complexes is $P2_1$ with unit cell
12
13 parameters of approximately $a=136 \text{ \AA}$, $b=301 \text{ \AA}$, $c=145 \text{ \AA}$ and $b=113$ (Table S3 in Supporting
14
15 Information). Datasets were collected using synchrotron radiation at the X06SA-beamline in
16
17 SLS/Villingen/Switzerland at $\lambda=1.0 \text{ \AA}$. X-ray intensities and data reduction were evaluated by
18
19 using the program package XDS.⁷⁶ The anisotropy of diffraction was corrected by comparing
20
21 observed and calculated structure amplitudes by the program CNS (including a bulk solvent
22
23 correction).⁷⁷ Electron density maps were improved by averaging and back transforming the
24
25 reflections 10 times over the two fold non-crystallographic symmetry axis using the program
26
27 package MAIN.⁷⁸ Conventional crystallographic rigid body and positional refinements were
28
29 carried out with CNS using coordinates of the yeast 20S proteasome structure (RCSB; 1RYP) as
30
31 a starting model.⁴⁵ Model building including the distinct ligands was performed with the program
32
33 COOT and final TLS refinement was carried out in REFMAC5. Apart from the bound inhibitor
34
35 molecules, structural changes were only noted in the specificity pockets. Temperature factor
36
37 refinement indicates full occupancies of all inhibitor binding sites. All models were completed
38
39 with final R_{free} values below 22.7% and root-mean-square deviation (rmsd) bond and angle
40
41 values of lower than 0.005 \AA and 0.9° , respectively (Table S3).
42
43
44
45
46
47
48
49

50 ASSOCIATED CONTENT

51
52 Supporting Information Available: Supplementary figures S1-S2, supplementary tables S1-S4,
53
54 scheme for the synthesis of compounds **3-6**, experimental procedures for the synthesis of
55
56
57
58
59
60

1
2
3 compounds **5a-d** and **6a-c**, copies of NMR spectra. This material is available free of charge via
4
5 the Internet at <http://pubs.acs.org>.
6
7

8
9 PDB ID Codes: yeast proteasome:**3a** (4JSU); yeast proteasome:**4a** (4JT0); yeast proteasome:**4e**
10
11 (4JSQ)
12
13

14 15 16 17 18 **AUTHOR INFORMATION**

19 20 21 Corresponding Authors Information

22
23
24 *Phone: + 33 2 23 23 57 33. Fax + 33 2 23 23 69 55. E-mail: joelle.vidal@univ-rennes1.fr
25

26
27 *Phone: +33 1 44 27 50 78. Fax: 33 1 44 27 51 40. E-mail: michele.reboud@upmc.fr
28
29

30 31 **Notes**

32
33 The authors declare no competing financial interest.
34
35
36
37

38 39 **ACKNOWLEDGMENTS**

40
41
42 X. M. received financial support from the Ministère de l'Enseignement Supérieur et de la
43
44 Recherche. We thank Prof. Michel Morange (Ecole Normale Supérieure and UPMC, Paris) for
45
46 fruitful discussions. This study was financed by grant n° 14999 from the 'Association Française
47
48 contre les Myopathies' (AFM) and the German-Israeli Foundation for Scientific Research and
49
50 Development (GIF 23 1102/2010 to M.G.).
51
52
53

54 55 **ABBREVIATIONS USED**

56
57
58
59
60

1
2
3 Ahx, aminohexanoic; AMC, 7-amino-4-methylcoumarin; ChT-L, chymotrypsin-like; EDC, 1-
4 Ethyl-3-(3-dimethylaminopropyl)carbodiimide, IFN- γ , interferon gamma; HOBt,
5 hydroxybenzotriazole; MES, morpholinoethane sulfonate; β NA, *beta*-naphthylamine; PA, post-
6 acid; Su, succinimydyl; Suc, succinyl; RPMI, Roswell Park Memorial Institute medium; T-L,
7 trypsin-like
8
9
10
11

12 13 14 REFERENCES

15
16
17 (1) Borissenko, L.; Groll, M., 20S proteasome and its inhibitors: Crystallographic knowledge
18 for drug development. *Chem. Rev.* **2007**, *107*, 687-717.
19

20
21
22 (2) Meiners, S.; Ludwig, A.; Stangl, V.; Stangl, K., Proteasome inhibitors: Poisons and
23 remedies. *Med. Res. Rev.* **2008**, *28*, 309-327.
24
25

26
27
28 (3) Richardson, P. G.; Mitsiades, C.; Hideshima, T.; Anderson, K. C., Bortezomib:
29 proteasome inhibition as an effective anticancer therapy. *Annu. Rev. Med.* **2006**, *57*, 33-47.
30
31

32
33
34 (4) Genin, E.; Reboud-Ravaux, M.; Vidal, J., Proteasome inhibitors: Recent advances and
35 new perspectives in medicinal chemistry. *Curr. Top. Med. Chem.* **2010**, *10*, 232-256.
36
37

38
39
40 (5) Adams, J.; Kauffman, M., Development of the proteasome inhibitor Velcade
41 (bortezomib). *Cancer Invest.* **2004**, *22*, 304-311.
42
43

44
45 (6) Groll, M.; Berkers, C. R.; Ploegh, H. L.; Ovaa, H., Crystal structure of the boronic acid-
46 based proteasome inhibitor bortezomib in complex with the yeast 20S proteasome. *Structure*
47
48
49 **2006**, *14*, 451-456.
50

51
52
53 (7) Chauhan, D.; Hideshima, T.; Anderson, K. C., Proteasome inhibition in multiple
54 myeloma: Therapeutic implication. *Annu. Rev. Pharmacol. Toxicol.* **2005**, *45*, 465-476.
55
56
57
58
59
60

1
2
3 (8) Argyriou, A. A.; Iconomou, G.; Kalofonos, H. P., Bortezomib-induced peripheral
4 neuropathy in multiple myeloma: a comprehensive review of the literature. *Blood* **2008**, *112*,
5 1593-1599.
6
7

8
9
10
11 (9) Demo, S. D.; Kirk, C. J.; Aujay, M. A.; Buchholz, T. J.; Dajee, M.; Ho, M. N.; Jiang, J.;
12 Laidig, G. J.; Lewis, E. R.; Parlati, F.; Shenk, K. D.; Smyth, M. S.; Sun, C. M.; Vallone, M. K.;
13 Woo, T. M.; Molineaux, C. J.; Bennett, M. K., Antitumor activity of PR-171, a novel irreversible
14 inhibitor of the proteasome. *Cancer Res.* **2007**, *67*, 6383-6391.
15
16
17

18
19
20
21 (10) Naujokat, C.; Fuchs, D.; Berges, C., Adaptive modification and flexibility of the
22 proteasome system in response to proteasome inhibition. *BBA Mol. Cell Res.* **2007**, *1773*, 1389-
23 1397.
24
25
26

27
28
29 (11) O'Connor, O. A.; Stewart, A. K.; Vallone, M.; Molineaux, C. J.; Kunkel, L. A.;
30 Gerecitano, J. F.; Orłowski, R. Z., A phase 1 dose escalation study of the safety and
31 pharmacokinetics of the novel proteasome inhibitor carfilzomib (PR-171) in patients with
32 hematologic malignancies. *Clin. Cancer Res.* **2009**, *15*, 7085-7091.
33
34
35
36

37
38
39 (12) Potts, B. C.; Albitar, M. X.; Anderson, K. C.; Baritaki, S.; Berkers, C.; Bonavida, B.;
40 Chandra, J.; Chauhan, D.; Cusack, J. C.; Fenical, W.; Ghobrial, I. M.; Groll, M.; Jensen, P. R.;
41 Lam, K. S.; Lloyd, G. K.; McBride, W.; McConkey, D. J.; Miller, C. P.; Neuteboom, S. T. C.;
42 Oki, Y.; Ovaa, H.; Pajonk, F.; Richardson, P. G.; Roccaro, A. M.; Sloss, C. M.; Spear, M. A.;
43 Valashi, E.; Younes, A.; Palladino, M. A., Marizomib, a proteasome inhibitor for all seasons:
44 Preclinical profile and a framework for clinical trials. *Curr. Cancer Drug Targets* **2011**, *11*, 254-
45 284.
46
47
48
49
50
51
52
53
54
55
56
57
58
59
60

1
2
3 (13) Kupperman, E.; Lee, E. C.; Cao, Y.; Bannerman, B.; Fitzgerald, M.; Berger, A.; Yu, J.;
4
5 Yang, Y.; Hales, P.; Bruzzese, F.; Liu, J.; Blank, J.; Garcia, K.; Tsu, C.; Dick, L.; Fleming, P.;
6
7 Yu, L.; Manfredi, M.; Rolfe, M.; Bolen, J., Evaluation of the proteasome inhibitor MLN9708 in
8
9 preclinical models of human cancer. *Cancer Res.* **2010**, *70*, 1970-1980.
10
11

12
13 (14) Zhou, H.-J.; Aujay, M. A.; Bennett, M. K.; Dajee, M.; Demo, S. D.; Fang, Y.; Ho, M. N.;
14
15 Jiang, J.; Kirk, C. J.; Laidig, G. J.; Lewis, E. R.; Lu, Y.; Muchamuel, T.; Parlati, F.; Ring, E.;
16
17 Shenk, K. D.; Shields, J.; Shwonek, P. J.; Stanton, T.; Sun, C. M.; Sylvain, C.; Woo, T. M.;
18
19 Yang, J., Design and synthesis of an orally bioavailable and selective peptide epoxyketone
20
21 proteasome inhibitor (PR-047). *J. Med. Chem.* **2009**, *52*, 3028-3038.
22
23
24
25

26 (15) Piva, R.; Ruggeri, B.; Williams, M.; Costa, G.; Tamagno, I.; Ferrero, D.; Giai, V.; Coscia,
27
28 M.; Peola, S.; Massaia, M.; Pezzoni, G.; Allievi, C.; Pescalli, N.; Cassin, M.; di Giovine, S.;
29
30 Nicoli, P.; de Feudis, P.; Strepponi, I.; Roato, I.; Ferracini, R.; Bussolati, B.; Camussi, G.; Jones-
31
32 Bolin, S.; Hunter, K.; Zhao, H.; Neri, A.; Palumbo, A.; Berkers, C.; Ovaa, H.; Bernareggi, A.;
33
34 Inghirami, G., CEP-18770: a novel, orally active proteasome inhibitor with a tumor-selective
35
36 pharmacologic profile competitive with bortezomib. *Blood* **2008**, *111*, 2765-2775.
37
38
39
40

41 (16) Groll, M.; Huber, R.; Potts, B. C. M., Crystal structures of salinosporamide A (NPI-0052)
42
43 and B (NPI-0047) in complex with the 20S proteasome reveal important consequences of beta -
44
45 lactone ring opening and a mechanism for irreversible binding. *J. Am. Chem. Soc.* **2006**, *128*,
46
47 5136-5141.
48
49
50

51 (17) Gräwert, M. A.; Groll, M., Exploiting nature's rich source of proteasome inhibitors as
52
53 starting points in drug development. *Chem. Commun.* **2012**, *48*, 1364-1378.
54
55
56
57
58
59
60

1
2
3 (18) Koguchi, Y.; Kohno, J.; Nishio, M.; Takahashi, K.; Okuda, T.; Ohnuki, T.; Komatsubara,
4 S., TMC-95A, B, C, and D, novel proteasome inhibitors produced by *Apiospora montagnei* Sacc.
5
6 TC 1093. Taxonomy, production, isolation, and biological activities. *J. Antibiot.* **2000**, *53*, 105-
7
8 109.
9

10
11
12 (19) Groll, M.; Götz, M.; Kaiser, M.; Weyher, E.; Moroder, L., TMC-95-based inhibitor
13 design provides evidence for the catalytic versatility of the proteasome. *Chem. Biol.* **2006**, *13*,
14
15 607-614.
16
17

18
19
20 (20) Lin, S.; Yang, Z.-Q.; Kwok, B. H. B.; Koldobskiy, M.; Crews, C. M.; Danishefsky, S. J.,
21 Total synthesis of TMC-95A and -B via a new reaction leading to Z-enamides. Some preliminary
22 findings as to SAR. *J. Am. Chem. Soc.* **2004**, *126*, 6347-6355.
23
24
25

26
27 (21) Kaiser, M.; Groll, M.; Siciliano, C.; Assfalg-Machleidt, I.; Weyher, E.; Kohno, J.;
28 Milbradt, A. G.; Renner, C.; Huber, R.; Moroder, L., Binding mode of TMC-95A analogues to
29 eukaryotic 20S proteasome. *ChemBioChem* **2004**, *5*, 1256-1266.
30
31
32

33
34 (22) Basse, N.; Piguel, S.; Papapostolou, D.; Ferrier-Berthelot, A.; Richy, N.; Pagano, M.;
35 Sarthou, P.; Sobczak-Thépot, J.; Reboud-Ravaux, M.; Vidal, J., Linear TMC-95-based
36 proteasome inhibitors. *J. Med. Chem.* **2007**, *50*, 2842-2850.
37
38
39

40
41 (23) Groll, M.; Gallastegui, N.; Maréchal, X.; Le Ravalec, V.; Basse, N.; Richy, N.; Genin, E.;
42 Huber, R.; Moroder, L.; Vidal, J.; Reboud-Ravaux, M., 20S Proteasome inhibition: designing
43 noncovalent linear peptide mimics of the natural product TMC-95A. *ChemMedChem* **2010**, 1701-
44
45 1705.
46
47
48
49
50
51
52
53
54
55
56
57
58
59
60

1
2
3 (24) Furet, P.; Imbach, P.; Fürst, P.; Lang, M.; Noorani, M.; Zimmermann, J.; Garcia-
4 Echeverria, C., Modeling of the binding mode of a non-covalent inhibitor of the 20S proteasome.
5 Application to structure-based analogue design. *Bioorg. Med. Chem. Lett.* **2001**, *11*, 1321-1324.
6
7

8
9
10
11 (25) Furet, P.; Imbach, P.; Noorani, M.; Koeppler, J.; Laumen, K.; Lang, M.; Guagnano, V.;
12 Fürst, P.; Roesel, J.; Zimmermann, J.; Garcia Echeverria, C., Entry into a new class of potent
13 proteasome inhibitors having high antiproliferative activity by structure-based design. *J. Med.*
14 *Chem.* **2004**, *47*, 4810-4813.
15
16
17

18
19
20
21 (26) Basse, N.; Papapostolou, D.; Pagano, M.; Reboud-Ravaux, M.; Bernard, E.; Felten, A.-S.;
22 Vanderesse, R., Development of lipopeptides for inhibiting 20S proteasomes. *Bioorg. Med.*
23 *Chem. Lett.* **2006**, *16*, 3277-3281.
24
25
26
27

28
29 (27) Formicola, L.; Maréchal, X.; Basse, N.; Bouvier-Durand, M.; Bonnet-Delpon, D.;
30 Milcent, T.; Reboud-Ravaux, M.; Onger, S., Novel fluorinated pseudopeptides as proteasome
31 inhibitors. *Bioorg. Med. Chem. Lett.* **2009**, *19*, 83-86.
32
33
34
35
36

37 (28) Blackburn, C.; Gigstad, K. M.; Hales, P.; Garcia, K.; Jones, M.; Bruzzese, F. J.; Barrett,
38 C.; Liu, J. X.; Soucy, T. A.; Sappal, D. S.; Bump, N.; Olhava, E. J.; Fleming, P.; Dick, L. R.; Tsu,
39 C.; Sintchak, M. D.; Blank, J. L., Characterization of a new series of non-covalent proteasome
40 inhibitors with exquisite potency and selectivity for the 20S beta 5-subunit. *Biochem. J.* **2010**,
41 *430*, 461-476.
42
43
44
45
46
47
48

49 (29) Blackburn, C.; Barrett, C.; Blank, J. L.; Bruzzese, F. J.; Bump, N.; Dick, L. R.; Fleming,
50 P.; Garcia, K.; Hales, P.; Hu, Z. G.; Jones, M.; Liu, J. X.; Sappal, D. S.; Sintchak, M. D.; Tsu, C.;
51 Gigstad, K. M., Optimization of a series of dipeptides with a P3 threonine residue as non-
52
53
54
55
56
57
58
59
60

1
2
3 covalent inhibitors of the chymotrypsin-like activity of the human 20S proteasome. *Bioorg. Med.*
4
5 *Chem. Lett.* **2010**, *20*, 6581-6586.

6
7
8
9 (30) Gallastegui, N.; Beck, P.; Arciniega, M.; Huber, R.; Hillebrand, S.; Groll, M.,
10
11 Hydroxyureas as Noncovalent Proteasome Inhibitors. *Angew. Chem. Int. Ed.* **2012**, *51*, 247-249.

12
13
14 (31) Basse, N.; Montes, M.; Maréchal, X.; Qin, L.; Bouvier-Durand, M.; Genin, E.; Vidal, J.;
15
16 Villoutreix, B. O.; Reboud-Ravaux, M., Novel organic proteasome inhibitors identified by virtual
17
18 and *in vitro* screening. *J. Med. Chem.* **2010**, *53*, 509-513.

19
20
21
22 (32) Huber, E. M.; Groll, M., Inhibitors for the immuno- and constitutive proteasome: Current
23
24 and future trends in drug development. *Angew. Chem. Int. Ed.* **2012**, *51*, 8708-8720.

25
26
27
28 (33) Wang, J.; Maldonado, M. A., The ubiquitin-proteasome system and its role in
29
30 inflammatory and autoimmune diseases. *Cell Mol. Immunol* **2006**, *3*, 255-261.

31
32
33 (34) Skaug, B.; Jiang, X.; Chen, Z. J., The role of ubiquitin in NF-kappaB regulatory
34
35 pathways. *Annu. Rev. Biochem.* **2009**, *78*, 769-796.

36
37
38
39 (35) Bonuccelli, G.; Sotgia, F.; Capozza, F.; Gazzero, E.; Minetti, C.; Lisanti, M. P.,
40
41 Localized treatment with a novel FDA-approved proteasome inhibitor blocks the degradation of
42
43 dystrophin and dystrophin-associated proteins in mdx mice. *Cell Cycle* **2007**, *6*, 1242-1248.

44
45
46
47 (36) Azakir, B. A.; Di Fulvio, S.; Kinter, J.; Sinnreich, M., Proteasomal Inhibition Restores
48
49 Biological Function of Mis-sense Mutated Dysferlin in Patient-derived Muscle Cells. *J. Biol.*
50
51 *Chem.* **2012**, *287*, 10344-10354.

52
53
54
55 (37) Jagoe, R. T.; Goldberg, A. L., What do we really know about the ubiquitin-proteasome
56
57 pathway in muscle atrophy? *Curr. Opin. Clin. Nutr. Metab. Care* **2001**, *4*, 183-190.
58
59
60

1
2
3 (38) Lindenthal, C.; Weich, N.; Chia, Y. S.; Heussler, V.; Klinkert, M. Q., The proteasome
4 inhibitor MLN-273 blocks exoerythrocytic and erythrocytic development of *Plasmodium*
5 parasites. *Parasitology* **2005**, *131*, (Pt 1), 37-44.
6
7

8
9
10
11 (39) Li, H.; Ponder, E.L.; Verdoes, M.; Asbjornsdottir, K.H.; Deu, E.; Edgington, L.E.; Lee,
12 J.T.; Kirk, C.J.; Demo, S.D.; Williamson, K.C.; Bogyo, M. Validation of the proteasome as a
13 therapeutic target in *Plasmodium* using an epoxyketone inhibitor with parasite-specific toxicity.
14
15
16
17
18
19
20
21
22
23
24
25
26
27
28
29
30
31
32
33
34
35
36
37
38
39
40
41
42
43
44
45
46
47
48
49
50
51
52
53
54
55
56
57
58
59
60

(40) Li, Z.; Zou, C. B.; Yao, Y.; Hoyt, M. A.; McDonough, S.; Mackey, Z. B.; Coffino, P.;
Wang, C. C., An easily dissociated 26 S proteasome catalyzes an essential ubiquitin-mediated
protein degradation pathway in *Trypanosoma brucei*. *J. Biol. Chem.* **2002**, *277*, 15486-15498.

(41) Steverding, D., The proteasome as a potential target for chemotherapy of African
trypanosomiasis. *Drug Dev. Res.* **2007**, *68*, 205-212.

(42) Steverding, D.; Wang, X.; Potts, B. C.; Palladino, M. A., Trypanocidal activity of beta-
lactone-gamma-lactam proteasome inhibitors. *Planta Med.* **2012**, *78*, 131-134.

(43) Lin, G.; Li, D.; de Carvalho, L. P.; Deng, H.; Tao, H.; Vogt, G.; Wu, K.; Schneider, J.;
Chidawanyika, T.; Warren, J. D.; Li, H.; Nathan, C., Inhibitors selective for mycobacterial versus
human proteasomes. *Nature* **2009**, *461*, 621-626.

(44) Lander, G. C.; Estrin, E.; Matyskiela, M. E.; Bashore, C.; Nogales, E.; Martin, A.,
Complete subunit architecture of the proteasome regulatory particle. *Nature* **2012**, *482*, 186-191.

(45) Groll, M.; Ditzel, L.; Löwe, J.; Stock, D.; Bochtler, M.; Bartunik, H. D.; Huber, R.,
Structure of 20S proteasome from yeast at 2.4 Å resolution. *Nature* **1997**, *386*, 463-471.

1
2
3 (46) Unno, M.; Mizushima, T.; Morimoto, Y.; Tomisugi, Y.; Tanaka, K.; Yasuoka, N.;
4
5 Tsukihara, T., The structure of the mammalian 20S proteasome at 2.75 Å resolution. *Structure*
6
7 **2002**, *10*, 609-618.
8
9

10
11 (47) Huber, E. M.; Basler, M.; Schwab, R.; Heinemeyer, W.; Kirk, C. J.; Groettrup, M.; Groll,
12
13 M., Immuno- and constitutive proteasome crystal structures reveal differences in substrate and
14
15 inhibitor specificity. *Cell* **2012**, *148*, 727-738.
16
17

18
19 (48) Frentzel, S.; Pesold-Hurt, B.; Seelig, A.; Kloetzel, P.-M., 20 S proteasomes are assembled
20
21 via distinct precursor complexes processing of LMP2 and LMP7 proproteins takes place in 13-16
22
23 S preproteasome complexes. *J. Mol. Biol.* **1994**, *236*, 975-981.
24
25

26
27 (49) Ortiz-Navarrete, V.; Seelig, A.; Gernold, M.; Frentzel, S.; Kloetzel, P. M.; Hammerling,
28
29 G. J., Subunit of the '20S' proteasome (multicatalytic proteinase) encoded by the major
30
31 histocompatibility complex. *Nature* **1991**, *353*, 662-664.
32
33

34
35 (50) Kisselev, A. F.; Callard, A.; Goldberg, A. L., Importance of the different proteolytic sites
36
37 of the proteasome and the efficacy of inhibitors varies with the protein substrate. *J. Biol. Chem.*
38
39 **2006**, *281*, 8582-8590.
40
41

42
43 (51) Britton, M.; Lucas, M. M.; Downey, S. L.; Screen, M.; Pletnev, A. A.; Verdoes, M.;
44
45 Tokhunts, R. A.; Amir, O.; Goddard, A. L.; Pelphrey, P. M.; Wright, D. L.; Overkleeft, H. S.;
46
47 Kisselev, A. F., Selective inhibitor of proteasome's caspase-like sites sensitizes cells to specific
48
49 inhibition of chymotrypsin-like sites. *Chem. Biol.* **2009**, *16*, 1278-1289.
50
51

52
53 (52) Screen, M.; Britton, M.; Downey, S. L.; Verdoes, M.; Voges, M. J.; Blom, A. E.; Geurink,
54
55 P. P.; Risseuw, M. D.; Florea, B. I.; van der Linden, W. A.; Pletnev, A. A.; Overkleeft, H. S.;
56
57
58
59
60

1
2
3 Kisselev, A. F., Nature of pharmacophore influences active site specificity of proteasome
4 inhibitors. *J. Biol. Chem.* **2010**, *285*, 40125-40134.
5
6
7

8
9 (53) Mirabella, A. C.; Pletnev, A. A.; Downey, S. L.; Florea, B. I.; Shabaneh, T. B.; Britton,
10 M.; Verdoes, M.; Filippov, D. V.; Overkleeft, H. S.; Kisselev, A. F., Specific cell-permeable
11 inhibitor of proteasome trypsin-like sites selectively sensitizes myeloma cells to bortezomib and
12 carfilzomib. *Chem. Biol.* **2011**, *18*, 608-618.
13
14
15
16
17

18
19 (54) Glenn, R. J.; Pemberton, A. J.; Royle, H. J.; Spackman, R. W.; Smith, E.; Jennifer Rivett,
20 A.; Steverding, D., Trypanocidal effect of alpha',beta'-epoxyketones indicates that trypanosomes
21 are particularly sensitive to inhibitors of proteasome trypsin-like activity. *Int. J. Antimicrob.*
22 *Agents* **2004**, *24*, 286-289.
23
24
25
26
27

28
29 (55) Mammen, M.; Choi, S.-K.; Whitesides, G. M., Polyvalent interactions in biological
30 systems: implications for design and use of multivalent ligands and inhibitors. *Angew. Chem., Int.*
31 *Ed.* **1998**, *37*, 2754-2794.
32
33
34
35
36

37 (56) Moroder, L., Application of the principle of polyvalency to protease inhibition. In *Modern*
38 *Biopharmaceuticals*, Knäblein, J., Ed. Wiley-VCH: **2005**; Vol. 2, pp 395-417.
39
40
41

42
43 (57) Loidl, G.; Groll, M.; Musiol, H.-J.; Huber, R.; Moroder, L., Bivalency as a principle for
44 proteasome inhibition. *Proc. Natl. Acad. Sci. U. S. A.* **1999**, *96*, 5418-5422.
45
46
47

48 (58) Loidl, G.; Groll, M.; Musiol, H.-J.; Ditzel, L.; Huber, R.; Moroder, L., Bifunctional
49 inhibitors of the trypsin-like activity of eukaryotic proteasomes. *Chem. Biol.* **1999**, *6*, 197-204.
50
51
52
53
54
55
56
57
58
59
60

1
2
3 (59) Maréchal, X.; Pujol, A.; Richey, N.; Genin, E.; Basse, N.; Reboud-Ravaux, M.; Vidal, J.,
4
5 Noncovalent inhibition of 20S proteasome by pegylated dimerized inhibitors. *Eur. J. Med. Chem.*
6
7 **2012**, *52*, 322-327.
8
9

10
11 (60) French, A. C.; Thompson, A. L.; Davis, B. G., High-purity discrete PEG-oligomer
12
13 crystals allow structural insight. *Angew. Chem., Int. Ed.* **2009**, *48*, 1248-1252.
14
15

16
17 (61) Groll, M.; Heinemeyer, W.; Jäger, S.; Ullrich, T.; Bochtler, M.; Wolf, D. H.; Huber, R.,
18
19 The catalytic sites of 20S proteasomes and their role in subunit maturation: a mutational and
20
21 crystallographic study. *Proc. Natl. Acad. Sci. U. S. A.* **1999**, *96*, 10976-10983.
22
23

24
25 (62) Jones, N. A.; Sikorski, P.; Atkins, E. D. T.; Hill, M. J., Nature and structure of once-
26
27 folded nylon 6 monodisperse oligoamides in lamellar crystals. *Macromolecules* **2000**, *33*, 4146-
28
29 4154.
30
31

32
33 (63) Hines, J.; Groll, M.; Fahnstock, M.; Crews, C. M., Proteasome inhibition by fellutamide
34
35 B induces nerve growth factor synthesis. *Chem. Biol.* **2008**, *15*, 501-512.
36
37

38
39 (64) Groll, M.; Schellenberg, B.; Bachmann, A. S.; Archer, C. R.; Huber, R.; Powell, T. K.;
40
41 Lindow, S.; Kaiser, M.; Dudler, R., A plant pathogen virulence factor inhibits the eukaryotic
42
43 proteasome by a novel mechanism. *Nature* **2008**, *452*, 755-758.
44
45

46
47 (65) Stein, M. L.; Beck, P.; Kaiser, M.; Dudler, R.; Becker, C. F. W.; Groll, M., One-shot
48
49 NMR analysis of microbial secretions identifies highly potent proteasome inhibitor. *Proc. Natl.*
50
51 *Acad. Sci. U. S. A.* **2012**, *109*, (45), 18367-18371.
52
53

54
55 (66) Stein, R. L.; Melandri, F.; Dick, L., Kinetic Characterization of the chymotryptic activity
56
57 of the 20S proteasome. *Biochemistry* **1996**, *35*, 3899-3908.
58
59
60

1
2
3 (67) Kessler, B. M.; Tortorella, D.; Altun, M.; Kisselev, A. F.; Fiebiger, E.; Hekking, B. G.;
4
5 Ploegh, H. L.; Overkleeft, H. S., Extended peptide-based inhibitors efficiently target the
6
7 proteasome and reveal overlapping specificities of the catalytic β -subunits. *Chem. Biol.* **2001**, *8*,
8
9 913-929.
10

11
12
13 (68) Steverding, D.; Spackman, R. W.; Royle, H. J.; Glenn, R. J., Trypanocidal activities of
14
15 trileucine methyl vinyl sulfone proteasome inhibitors. *Parasitol. Res.* **2005**, *95*, 73-76.
16
17

18
19 (69) Steverding, D.; Pemberton, A. J.; Royle, H.; Spackman, R. W.; Rivett, A. J., Evaluation of
20
21 the anti-trypanosomal activity of tyropeptin A. *Planta Med.* **2006**, *72*, 761-763.
22
23

24
25 (70) Steverding, D.; Baldisserotto, A.; Wang, X.; Marastoni, M., Trypanocidal activity of
26
27 peptidyl vinyl ester derivatives selective for inhibition of mammalian proteasome trypsin-like
28
29 activity. *Exp. Parasitol.* **2011**, *128*, 444-447.
30
31

32
33 (71) Lin, Y.-M.; Miller, M. J., Oxidation of primary amines to oxaziridines using molecular
34
35 oxygen (O_2) as the ultimate oxidant *J. Org. Chem.* **2001**, *66*, 8282-8285.
36
37

38
39 (72) Donati, D.; Morelli, C.; Porcheddu, A.; Taddei, M., New Polymer-Supported Reagent for
40
41 the Synthesis of β -Lactams in Solution *J. Org. Chem.* **2004**, *69*, 9316-9318.
42
43

44
45 (73) Doughty, M. B.; Chaurasia, C. S.; Li, K., Benextramine-neuropeptide Y receptor
46
47 interactions: contribution of the benzylic moieties to [3H]neuropeptide Y displacement activity *J.*
48
49 *Med. Chem.* **1993**, *36*, 272-279.
50

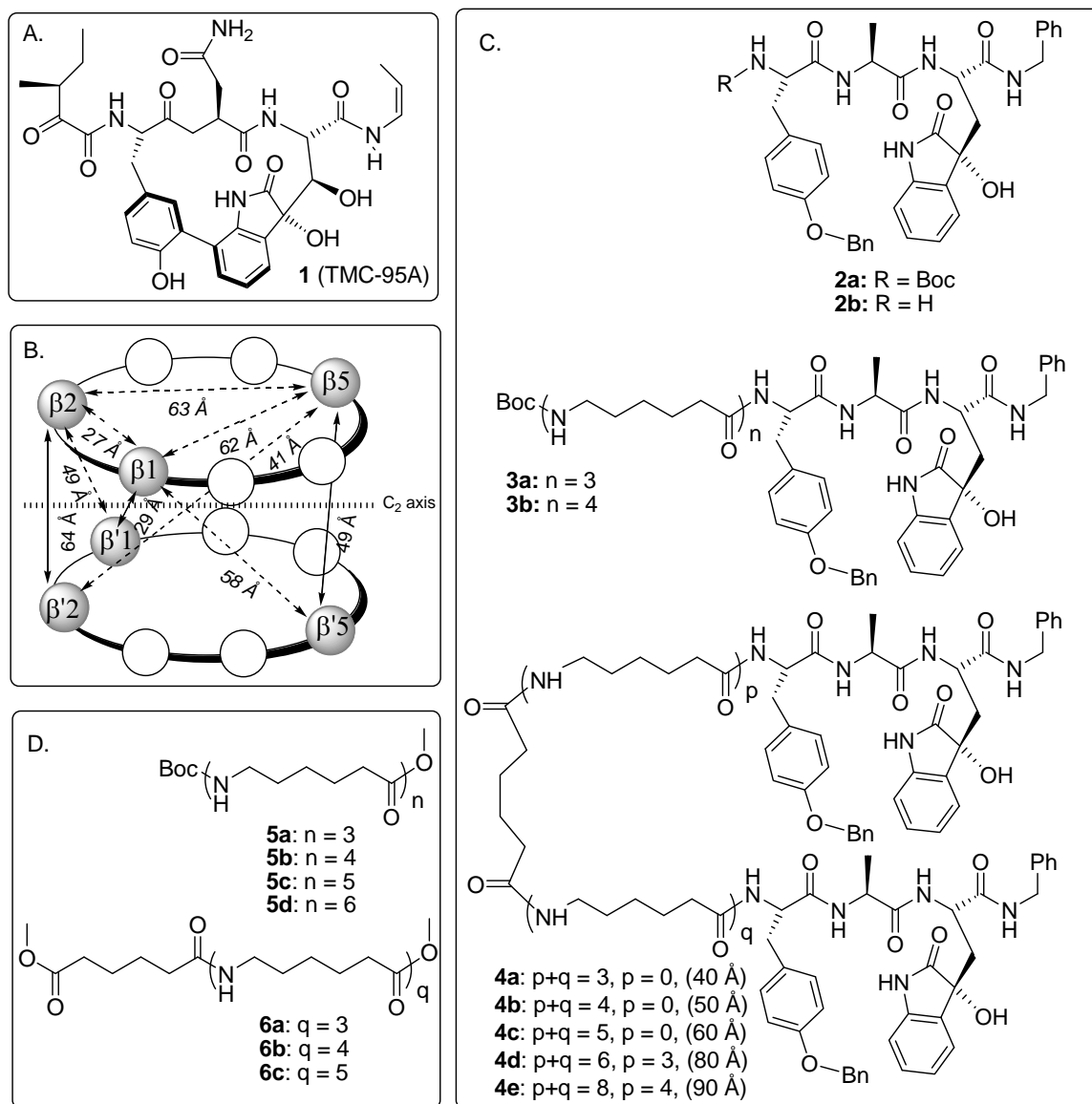
51
52 (74) Groll, M.; Huber, R., Purification, crystallization and X-ray analysis of the yeast 20S
53
54 proteasomes. *Methods Enzymol.* **2005**, *398*, (Part A), 329-336.
55
56
57
58
59
60

1
2
3 (75) Gallastegui, N.; Groll, M., Analysing properties of proteasome inhibitors using kinetic
4 and X-ray crystallographic studies. *Methods Mol. Biol.* **2012**, 832, 373-390.
5
6

7
8
9 (76) Kabsch, W., Automatic processing of rotation diffraction data from crystals of initially
10 unknown symmetry and cell constants. *J. Appl. Cryst.* **1993**, 26, 795-800.
11
12

13
14 (77) Brünger, A.; Adams, P.; Clore, G.; DeLano, W.; Gros, P.; Grosse-Kunstleve, R.; Jiang, J.;
15 Kuszewski, J.; Nilges, M.; Pannu, N.; Read, R.; Rice, L.; Simonson, T.; Warren, G.,
16 Crystallography & NMR system: A new software suite for macromolecular structure
17 determination. *Acta Crystallogr D Biol Crystallogr.* **1998**, 1, 905-921.
18
19
20
21
22

23
24 (78) Turk, D., Improvement of a programm for molecular graphics and manipulation of
25 electron densities and its application for protein structure determination. *Thesis* **1992**, Technische
26 Universität München.
27
28
29
30
31
32
33
34
35
36
37
38
39
40
41
42
43
44
45
46
47
48
49
50
51
52
53
54
55
56
57
58
59
60



42
43
44
45
46
47
48
49
50
51
52
53
54
55
56
57
58
59
60

Figure 1. (A). Structure of **1**. (B) Schematic representation of the yeast 20S proteasome, showing the dimer symmetry of β and β' stacked rings. The catalytic subunits are colored in grey. The distances between the catalytic Thr1 O^γ are derived from the X-ray structure.^{45,61} (C) Structures of studied inhibitors **2-4**; in the case of the dimeric compounds **4a-e**, the estimated length of the spacer in extended conformation is indicated. (D) Structures of the Ahx oligomers **5** and **6** used in the chemical synthesis of the studied inhibitors.

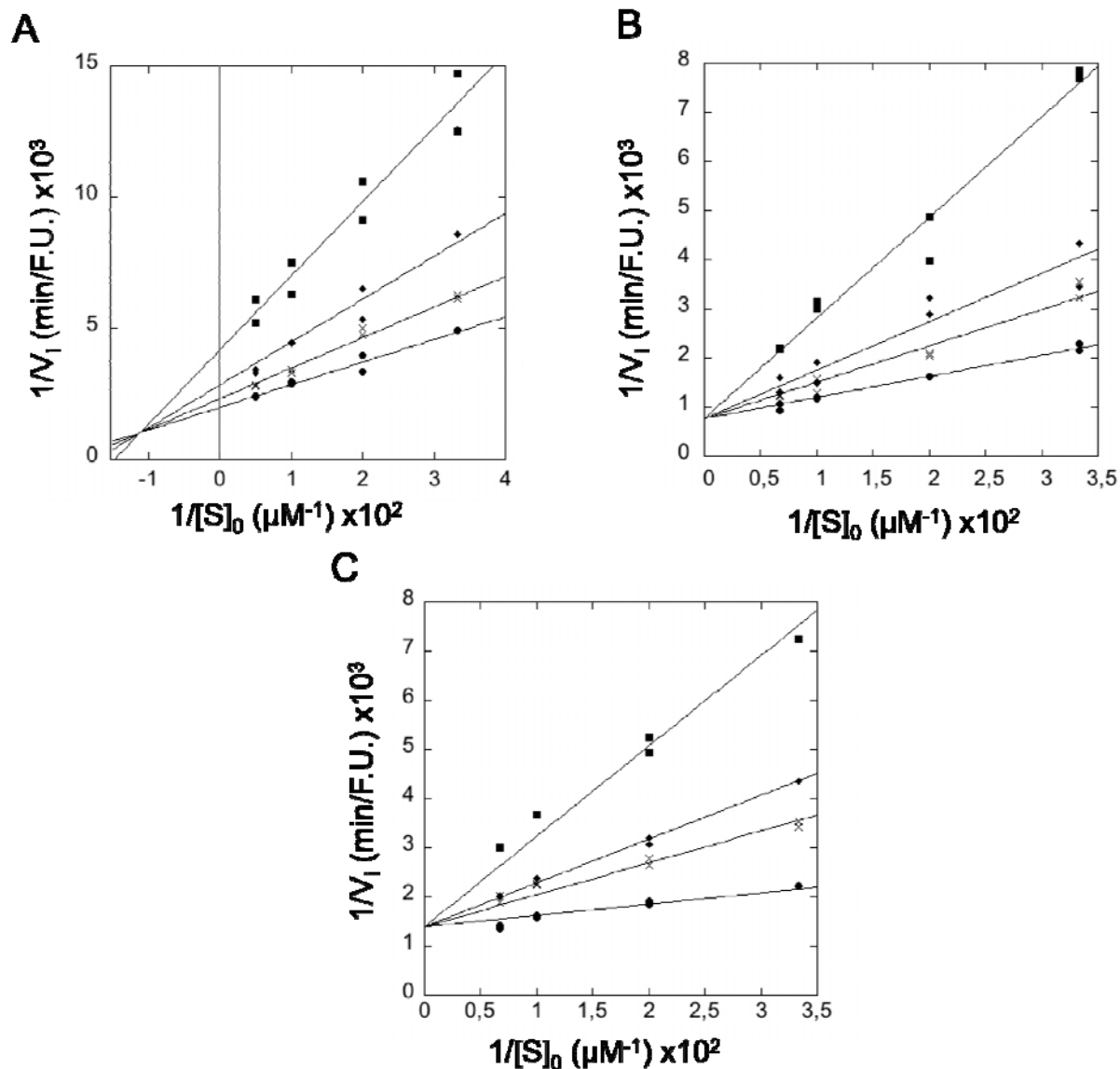


Figure 2. Double reciprocal Lineweaver-Burk plots for the inhibition of the ChT-L activity of human 20S proteasome by compound **2a** (A), **4b** (B) and **4e** (C) at pH 7.5 and 37 °C. [20S proteasome] $_0$ = 0.3 nM. Experimental points were fitted to equations 4 (A) and 3 (B, C). The inhibitor concentrations were: ● 0, X 10 μM , ◆ 25 μM , ■ 60 μM (**2a**, A); ● 0, X 0.01 μM , ◆ 0.03 μM , ■ 0.05 μM (**4b**, B); ● 0, X 0.01 μM , ◆ 0.02 μM , ■ 0.04 μM (**4e**, C); F. U., fluorescence arbitrary units.

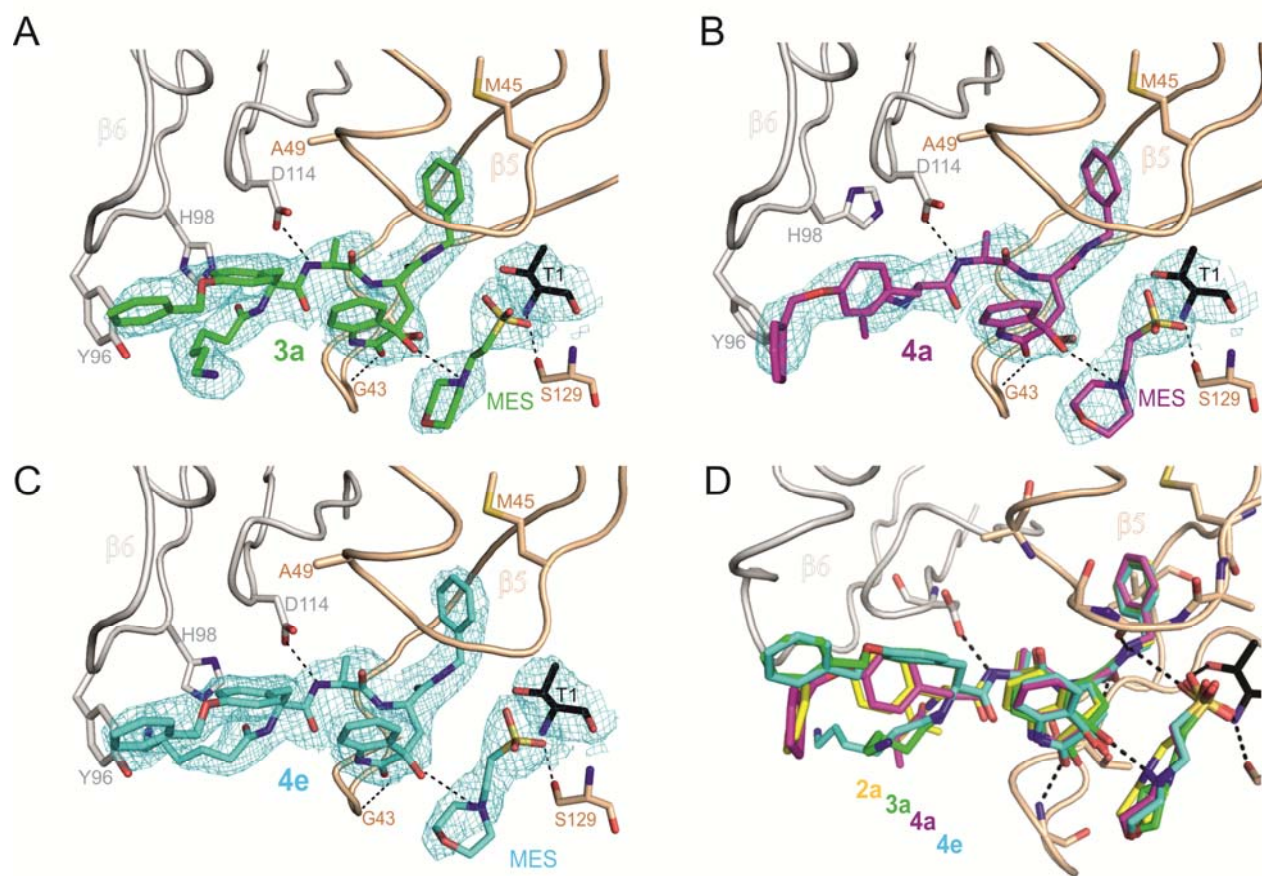


Figure 3. Crystal structures of the yeast 20S proteasome in complex with **3a** (A), **4a** (B) and **4e** (C). Subunits $\beta 5$ (beige) and $\beta 6$ (grey) are both shown in cartoon representations; the H-bonding network observed in this set of compounds are depicted in black dotted lines, whereas amino acids involved in complex formation are shown in stick forms. (D) Structural superposition of the compounds **2a**, **3a**, **4a** and **4e** (depicted in yellow, green, purple and blue respectively) bound to the ChT-L active site.

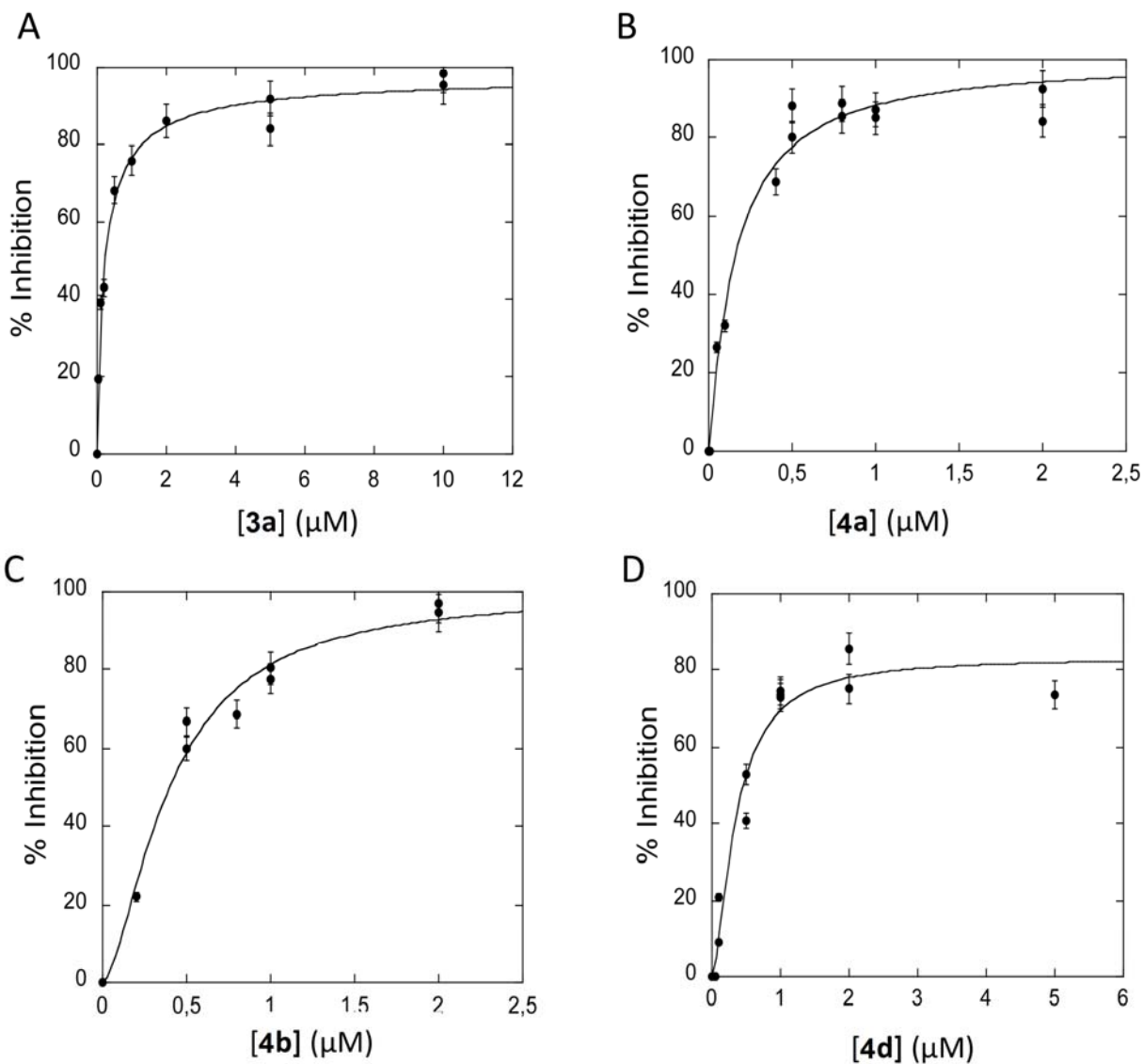
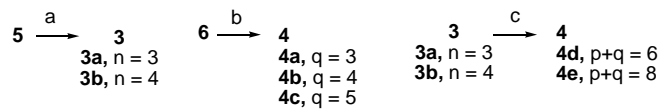


Figure 4. Inhibition profile for compounds **3a** (A), **4a** (B), **4b** (C) and **4d** (D) for the ChT-L

activity of cell-based proteasome-GloTM β 1 and β 5 assays after treatment of HEK-293 cells with the inhibitor for 2 h at 37°C. The experimental points were fitted to equation 4.

Scheme 1^a

^aReagents and conditions: (a) i. LiOH, H₂O, THF, rt then HCl, ii. EDC, HOBT, Et₃N, **2b** (1.2 eq.); (b) i. LiOH, H₂O, THF, rt then HCl, ii. EDC, HOBT, Et₃N, **2b** (2.5 eq.); (c) i. anhydrous HCl, MeOH, ii. ClCO(CH₂)₄COCl (0.5 eq.), Et₃N.

Table 1. Inhibition profile of the human constitutive 20S proteasome at pH 7.5 and 37°C.^a

Cpd	IC ₅₀ (nM) ^b			Mechanism of inhibition ^c	K _i (nM) ^d	K' _i (nM) ^d
	ChT-L	PA	T-L			
2a	3,190 ± 130	11,520 ± 470	7,160 ± 160	M	2,430 ± 260	5,030 ± 540
2b	11,600 ± 400	51,200 ± 500	ni	NC	24,500 ± 1900	24,500 ± 1900
3a	460 ± 14	4577 ± 50	867 ± 11	M	101 ± 10	316 ± 42
3b	707 ± 14	2560 ± 57	700 ± 23	M	67 ± 3	200 ± 37
4a	25.8 ± 1.1	590 ± 17	20.2 ± 1.0	C	10.3 ± 0.6	-
4b	25.9 ± 1.6	370 ± 8	12.4 ± 0.9	C	10.8 ± 0.7	-
4c	22.7 ± 1.6	448 ± 24	16.4 ± 1.2	C	11.4 ± 0.8	-
4d	19.1 ± 0.9	346 ± 18	14.8 ± 1.1	C	10.6 ± 1.1	-
4e	20.0 ± 0.1	336 ± 219	14.4 ± 2.5	C	6.0 ± 0.6	-
1^e	5.4	60	200	C	2.3	-

^a The inhibition was evaluated after 15 min incubation of the enzyme with the respective compounds before adding the appropriate fluorogenic substrate to evaluate the remaining activity (Suc-LLVY-AMC for ChT-L activity, Z-LLE-βNA for PA activity, and Boc-LRR-AMC for T-L activity).^b The IC₅₀ values were calculated by fitting the experimental data to the equations 1 or 2. ^c M, mixed; NC, non competitive; C, competitive. ^d K_i, inhibition constant for the dissociation of an EI complex; K'_i, inhibition constant for the dissociation of an ESI complex. ^e Human constitutive 20S proteasome.¹⁸

Table 2. Effects of different concentrations of compounds **3a**, **4a**, **4b** and **4d** on ChT-L activity of HEK-293 cells treated during 2 h by the inhibitors.^a

	IC ₅₀ (μM)	IC ₅₀ (μM) or % inhibition
	ChT-L	PA
Epoxomicin	0.026 ± 0.003	0.30 ± 0.05
MG132	0.009 ± 0.002	0.6 ± 0.1
2a	7.97 ± 0.15	16 ± 2
3a	0.252 ± 0.012	17.3 ± 0.5
4a	0.541 ± 0.169	40% (20 μM)
4b	0.756 ± 0.072	37% (10 μM)
4c	0.472 ± 0.028	25% (10 μM)
4d	0.476 ± 0.015	30% (10 μM)

^a The proteasomal activity was detected using the cell-based proteasome-Glo™ β5 assay.

Table of Contents Graphic

